Apomorphine Alters Prey-Catching Patterns in the Common Toad: Behavioral Experiments and 14C-2-Deoxyglucose Brain Mapping Studies

M. Glagow   J.-P. Ewert

Abteilung Neurobiologie, Fachbereich Biologie/Chemie, Universität Kassel, Kassel, Germany

Abstract

Previous studies on the dopaminergic modulation of visuomotor functions in amphibians showed that the dopamine agonist apomorphine (APO) alters prey-catching strategies. After systemic administration of APO in common toads *Bufo bufo,* prey-oriented turning and locomotion was attenuated whereas snapping toward prey was facilitated in a dose dependent manner. With systemic APO administration, toads which had previously been hunting, that is pursuing prey, behaved in a waiting position, that is sitting motionless and waiting for prey. This suggests that APO facilitates the ingestive component and inhibits the orientational and locomotory components of prey capture. To help unravel the cerebral sites of action of APO, the present study employs the 14C-2-deoxyglucose method to compare the rate of local glucose utilization in 41 brain structures. The retinal projection fields – e.g. superficial optic tectum, pretectal nuclei, and anterior dorsal thalamic nucleus – showed an elevation in glucose utilization due to APO-induced increases in retinal output. The medial tectal layers and the ventral striatum, both involved in visuomotor functions related to prey-oriented turning and locomotion, displayed APO-induced decreases in glucose utilization. APO-induced increases in glucose utilization were observed in the medial reticular formation and the hypoglossal nucleus which participate in the motor pattern generation of snapping. APO-induced increases in glucose utilization were also detected in the nucleus accumbens and the ventral tegmentum (mesolimbic system) as well as in the ventromedial pallium ('primordium hippocampi') and the septum, both of which belonging to the limbic system. These structures contribute to motivational level control and may be responsible for the APO-induced elevation of the snapping rate. Various other structures revealed APO-induced increases in glucose utilization. These structures include the olfactory bulb, lateral pallium, suprachiasmatic nucleus, nucleus of the periventricular organ, and the nucleus of the solitary tract. The lateral amygdala displayed APO-induced decreases in glucose utilization. The APO-induced alterations in local cerebral glucose utilization are evaluated with reference to the distribution of dopaminergic structures, and this is compared with similar data obtained in the rat by other authors. A neural network explaining the APO-induced behavioral syndrome in the common toad is discussed.

Introduction

In anuran amphibians, the primary visual response pathways that control prey orienting and snapping behaviors take advantage of ensembles of tectal cells [Ewert, 1987, 1997] whose axons travel in the tecto-bulbar and tecto-bul-

Prof. Dr. J.-P. Ewert
Abteilung Neurobiologie, FB19, Universität Gesamthochschule Kassel (GhK)
D–34109 Kassel (Germany)
Tel. +49 561 804 4784, Fax +49 561 804 4146
E-Mail ewertjp@aol.com

Abbreviations

A	anterior thalamic nucleus		LS	lateral septum		SCN	suprachiasmatic nucleus
AC	nucleus accumbence		mOB	medial main olfactory bulb		SNpr	substantia nigra pars reticulata
AL	nucleus amygdalae		mOT	medial optic tectum		SOL	nucleus of the solitary tract
AOS	accessory olfactory system		MRF	medullary medial reticular formation		sOT	snapping evoking area of OT
C	central thalamic nucleus					SP	spinal cord
dCB	dorsal cerebellum		MS	medial septum		TEG	tegmentum
dHYP	dorsal hypothalamus		N.V	nucleus of the nervous trigeminus		TS	torus semicircularis
dMP	dorsal medial pallium		N.VII	nucleus of the nervous facialis		Ttb	tractus tectobulbaris directus
dOT	dorsal optic tectum		N.XI	nucleus of the nervous accessorius		Ttb/s	tractus tectobulbaris et spinalis cruciatus
DP	dorsal pallium		N.XII	nucleus of the nervous hypoglossus			
dTEG	dorsal tegmentum					vCB	ventral cerebellum
Ea	anterior entopeduncular nucleus		NB/VLd	complex of the nucleus Bellonci and dorsal ventrolateral thalamic nucleus		vHYP	ventral hypothalamus
HAB	nucleus habenulae					VLv	ventral ventrolateral thalamic nucleus
HGL	hypoglossal nucleus						
HYP	hypothalamus		NPO	nucleus of the periventricular organ		VM	ventromedial thalamic nucleus
IST	nucleus isthmi					vMP	ventral medial pallium
La	lateral anterior thalamic nucleus		OT	optic tectum		vOB	ventral main olfactory bulb
Lpd	lateral posterodorsal pretectal thalamic nucleus		P	posterior pretectal thalamic nucleus		vOT	ventral optic tectum
						vSTR	ventral striatum
LPR	lateral prominence		pLP	posterior lateral pallium		vTEG	ventral tegmentum
Lpv	lateral posteroventral pretectal thalamic nucleus		PO	praeoptic area		I	1st ventricle
			R	retina		III	3rd ventricle

bar/spinal tracts to the appropriate motor pattern generating systems [Ingle, 1983; Grobstein et al., 1983; Satou and Ewert, 1985; Satou et al., 1985; Matsushima et al., 1989; Ewert et al., 1990]. These tectal releasing systems are controlled and modulated by striatal [Ewert, 1984; Finkenstädt, 1989; Patton and Grobstein, 1998a, b], pretectal [Ewert, 1968, 1987; Ewert et al., 1996], tegmental [Grobstein, 1991], preoptic/hypothalamic, and solitary/reticular [Weerasuriya, 1983; Székely et al., 1983] structures that contain dopaminergic cell bodies or fibers [González and Smeets, 1991].

As part of a research program to determine the role of dopamine in visuomotor function in amphibians [Ewert et al., 1999], we showed that the dopamine D_2/D_1-receptor agonist apomorphine (APO) modulates the components of prey-catching behavior in a dose dependent manner [for a characterization of D_1 and D_2 dopamine receptors in *Rana pipiens* see Chu et al., 1994]. In common toads *(Bufo bufo),* systemic administration of APO led, on one hand, to an attenuation in the activity of prey-oriented turning and locomotion, and, on the other hand, to a facilitation of prey snapping [Glagow and Ewert, 1997a]. After APO administration, common toads which had previously been hunting, that is pursuing prey, behaved in the manner of a frog that is waiting and sitting motionless until a prey object appears at snapping distance [Eibl-Eibesfeldt, 1951]. This suggests that APO facilitates the ingestive component and inhibits

the orientational and locomotory components of prey capture. It is possible that dopamine levels in specific brain areas could alter prey-catching strategies.

The APO-induced syndrome in common toads is comparable to oral behavioral stereotypies reported in other vertebrates after administration of APO, such as biting in the tortoise [Andersen et al., 1975], pecking in the pigeon [e.g. Dhawan et al., 1961; Burg et al., 1989], and sniffing, licking, and gnawing in rats [e.g. Ljungberg and Ungerstedt, 1977; McCulloch et al., 1982; Blackburn et al., 1992]. In mammals, APO-induced oral behaviors are generally discussed in connection with the mesolimbic dopaminergic system, arising from the ventral tegmental area and projecting mainly to the nucleus accumbens. Another system implicated in mammalian stereotyped oral behaviors is the dopaminergic nigrostriatal system, arising from the substantia nigra pars compacta and projecting to the corpus striatum [e.g. see Costall et al., 1972; Costall and Naylor, 1973; Creese and Iversen, 1975; Brown and Wolfson, 1978; McCulloch et al., 1982; Blackburn et al., 1992]. In amphibians, the striatum occupies the ventrolateral portion of the telencephalic hemisphere, and the nucleus accumbens lies in the ventromedial region of the telencephalic wall [Herrick, 1933; Hoffmann, 1973; Kokoros, 1973; Kicliter and Northcutt, 1975; Kicliter and Ebbesson, 1976; Kicliter, 1979; Northcutt and Kicliter, 1980; Parent and Dubé, 1983;

Wilczynski and Northcutt, 1983a, b]. Recent hodological, chemoarchitectonic, and developmental investigations on the basal ganglia organization in amphibians broadened our insight into the afferent and efferent connections of the striatum and the nucleus accumbens [González and Smeets, 1991; Marín et al., 1997a, b, c, 1998a, b]. The dopaminergic innervation of these brain structures has also been re-investigated [Marín et al., 1997d, e].

In the present investigation, we used the ^{14}C-2-deoxyglucose method [Sokoloff et al., 1977] in active toads to quantitatively map the metabolic activity in various structures of the neural macronetwork implicated in prey-catching releasing systems. The data are obtained from common toads *(Bufo bufo)* stimulated with moving prey or with non-prey stimuli either in the presence or absence of APO, respectively. In a control group, toads were treated with APO, but received no moving visual stimuli. Questions in this study focus on the: (1) causal relationships of the APO-induced behavioral syndrome with global changes in local cerebral glucose utilization, and (2) correlations between APO-induced alterations in local cerebral glucose utilization and the distribution of dopaminergic structures. Furthermore, comparisons of the data with results obtained in mammals are discussed.

Materials and Methods

Experimental Animals

The experimental animals were common toads of the species *Bufo bufo spinosus* obtained from a commercial dealer and kept in vivaria under controlled laboratory conditions at a temperature of 18 °C, a relative humidity of 50%, and a constant day(12 h)/night(12 h) circadian cycle. Each vivarium, measuring 60×30×30 cm in size, accommodated about 6 toads. A 5-cm thick segment of wet absorbent soft-foamed plastic material covered two thirds of the bottom. The remaining portion of the vivaria were filled with water and served as pools. Stones and bark were provided as shelter. The toads were fed on mealworms ad lib once a week.

A low level in blood glucose is a precondition of optimal uptake of ^{14}C-2-deoxyglucose [Young and Deutsch, 1980]. Collecting toad's cardiac blood we measured the blood glucose level from January through December using Rentascan® (Owen Mumfort), which yielded average ± SD glucose values of 50.8 ± 3.5 mg/100 ml in toads (n = 64) that had been food deprived for 7 days, and 57.7 ± 4.4 mg/100 ml in toads (n = 42) 30 min after ad lib feeding. We therefore food-deprived the toads for 7 days prior to the experiment in order to maintain a low blood glucose level. Animals were killed after the ^{14}C-2-deoxyglucose experiment with an overdose of MS222. MS222 does influence blood glucose level, such that an average ± SD glucose level of 86.6 ± 12.2 mg/100 ml, with peak levels up to 120 mg/100 ml, were measured in toads (n = 28) after an intralymphatic injection of a low dose of the anesthetic. The MS222 effect on blood glucose was not a problem in this study, however, as the anesthetic was administered only after the ^{14}C-2-deoxyglucose experiment was completed.
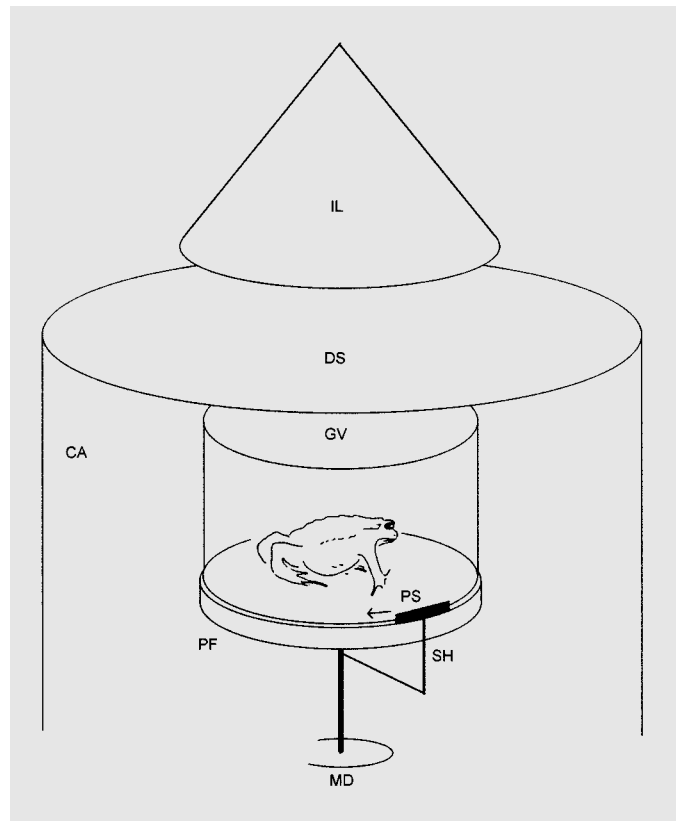
Fig. 1. Experimental procedure for stimulus presentation and measurements of toad's prey-catching patterns [after Ewert, 1984]. A black bar (PS) moving worm-like against a white background served as a prey dummy. This stimulus was moved mechanically around the toad sitting in a transparent cylindrical glass vessel (GV). The angular velocity of the stimulus – related to the center of rotation – was 7.6°/s. The distance between the prey stimulus and the glass vessel was 1 cm. CA = Cylindrical arena; DS = diffuse transparent screen; GV = glass vessel; IL = illumination; MD = electric motor device; PF = platform; PS = prey stimulus; SH = stimulus holder.

The experiments comply with the 'Principles of animal care', publication No. 85-23, revised 1985 of the National Institutes of Health and also with the laws of the Federal Republic of Germany in which the experiments were performed.

Stimulation Program and Experimental Groups

In the experimental groups, two types of visual stimuli were presented to the toads. The prey stimulus was a 4×28 mm black bar oriented parallel to the horizontal direction of movement ('worm' configuration). In pharmacologically untreated (i.e. normal) toads, this stimulus elicited prey-catching orienting behavior and snapping. A 28×4 mm black bar which was oriented perpendicular to the horizontal direction of movement ('antiworm' configuration) served as a non-prey stimulus; such a stimulus elicited no motor response in pharmacologically untreated toads. The stimulus(s)/background(b) contrast was C = (L$_b$−L$_s$)/(L$_b$+L$_s$) = 0.94, with L$_s$ = 1.3 cd × m$^{−2}$ and L$_b$ = 44 cd × m$^{−2}$. The experimental animal sat in a cylindrical transparent glass

Table 1. Experimental groups for ^{14}C-2DG experiments

Group	Visual stimulation	Stimulus frequency	APO administration	Orienting activity	Snapping activity	Number of toads
P	stimulated with prey	high	untreated	strong	weak	11
P*	stimulated with prey	low	treated	none	strong	13
N*	stimulated with non-prey	low	treated	none	very weak	10
C*	control, not stimulated	none	treated	none	none	6
C	control, not stimulated	none	untreated	none	none	5

vessel (29 cm diam.) in the center of a cylindrical platform (30 cm diam.) surrounded by a homogeneously white drum-shaped arena (fig. 1). In this procedure [Ewert, 1984], the stimulus was mechanically moved close to the edge of the platform in a circle around the vessel at a constant distance from the vessel and at a constant angular velocity of 7.6 deg/s (2 cm/s) during a 45 min experimental period. This period was interrupted by 2-min recovery pauses after each double circle in order to prevent habituation. After each double circle, the direction of movement was reversed.

We selected toads that responded to the prey stimulus with about 20 prey-catching reactions per 30 s, to eliminate variability in prey-catching motivation [cf. Wachowitz and Ewert, 1996]. Sequential orientational turning movements of the experimental animal in response to the circling stimulus were easily determined. The projection of the toad's tongue in an attempt to contact the stimulus counted as a snap; in all cases, the tongue hit the glass vessel. Five experimental groups were investigated (table 1). In the P-group, toads were stimulated with the prey-dummy and they received no APO; in the P*-group and N*-group, a prey or non-prey stimulus, respectively, was presented to the toad after administration of APO. In two other groups, toads were treated with APO (C*-group) or were untreated (C-group) in the absence of a moving visual stimulus. The P- and P*-groups are the main test groups; the N*-, C*-, and C-groups served as controls.

Drug Administration

A solution of apomorphine (APO) was injected intralymphatically, at a dose of 40 mg/kg body weight, one minute prior to the administration of ^{14}C-2-deoxyglucose. Dose/effect measurements in common toads (cf. fig. 2) previously have shown that this concentration is optimal to simultaneously suppress orientational turning behavior and facilitate snapping [Glagow and Ewert, 1997a]. Compared to birds and mammals, this effective dose of 40 mg/kg body wt. is relatively high and probably due to the lymphatic application of APO (poor lymphatic circulation and relatively weak access to the brain). The APO-induced behavioral effects started about 5 min following drug administration, and were maximal after 30 min, but faded after 50 min [see Glagow and Ewert, 1997a].

^{14}C-2DG Autoradiography

One minute prior to the 45-min stimulation session in the P-, P*-, N*-, C*-, or C-groups, 150 μCi/kg of [^{14}C]-2-deoxy-D-glucose (^{14}C-2DG, New England Nuclear) were injected into the caudal lymphatic sacs. Immediately after testing, the animals were deeply anaesthetized with an overdose of MS222 and perfused by a 25 ml solution consisting of 0.05 mol/l phosphate buffer, 0.6% NaCl, and 0.8% sucrose. Subse-

quently the animals were perfused by a 25 ml fixative containing 1.5% glutaraldehyde, 4% sucrose, and 1% dimethylsulfoxide in 0.05 molar phosphate buffer. The brains were carefully removed, immediately frozen at –30°C, and sectioned (40 μm) in a cryostat at –15°C. Sections were dried on a hot-plate at +60°C. We prepared autoradiographs from these transverse sections by exposing them with X-ray film (Kodak X-OMAT-MA2) in light-tight X-ray cassettes for 21 days.

The radioactivity served as an index of the ^{14}C-2DG uptake and thus the glucose utilization in the brain tissue required for the local cerebral energy metabolism which, in turn, correlates with neural activity [Sokoloff et al., 1977]. The tissue concentrations of ^{14}C were determined from their optical densities by comparing them to the optical densities of calibrated ^{14}C-metyl-metacrylate standards, which were exposed to the X-ray film at the same time as the sections. Brain sections were stained with cresyl violet. For methodological details we refer to Finkenstädt et al. [1985, 1986].

Computerized Densitometry

By means of a computer-aided densitometry system 'Automet' (unpublished), we determined the optical density of various structures in the autoradiographic images of the transverse brain sections. The autoradiographs and the counter-stained histological sections were precisely aligned. This provided a one-to-one correspondence between the functional activity revealed on the film and the anatomical site [for further details see Gallistel et al., 1982].

The image analyzing system Automet was developed in collaboration with the Department of Mathematics/Informatics at the University of Kassel. The main processing steps of the system are the following: The data of the autoradiographic images are read by a CCD videocamera and transformed into a graphic format (bit map coded as a 256 grey scale image) by means of a commercial software (screen machine). The developed image analyzing software is a MS-Windows application. It allows one to process the bit map data and to express these in false colors. During this procedure, the camera data are processed depending on the optical density of the autoradiographic images. A defined interval of each optical density is assigned (via standards) to an autoradiographic activity level and to a certain color. Thus, the experimenter obtains a 'reference table' that corresponds directly to an 'autoradiographic density table'.

Data Analysis

From each animal of the different experimental groups (P, P*, N*, C, and C*) the average ^{14}C-concentration value (^{14}C$_{P,P*,N*,C,C*}$) of the brain structures (obtained via ^{14}C-methyl-methacrylate standards) was related to the average ^{14}C-concentration value of a white-matter (wh)

reference structure $^{14}C_{wh}$ (e.g. $X_P = {}^{14}C_P/{}^{14}C_{wh}$). The standard reference structure, an area below the nucleus ventralis nervi octavi, showed no change in glucose utilization in response to either visual stimulation, motor activity or after administration of APO. The X values were calculated for a number of histological transverse sections on which the brain structure of interest appeared along its sagittal extension. The bilateral values of these brain sections in each toad were averaged, and these individual means were averaged to give the group mean X'. Thus, each subject will have the same weight in the final results, and a calculation of dispersion ($\pm SDM$) shows an estimate of the variance of the data (e.g. fig. 5A). The APO-induced changes in glucose utilization in a brain structure from toads exposed to the visual prey-stimulus is expressed by $X'_{P*;P}$ (%) = 100 $(X'_{P*}-X'_P)/X'_P$ (e.g. fig. 8A). Correspondingly, the differences in glucose utilization with respect to prey and non-prey stimuli in APO-treated toads are expressed by $X'_{P*;N*}$ (%) = 100 $(X'_{P*}-X'_{N*})/X'_{N*}$, and the control for the effects of APO in the absence of moving visual stimuli is expressed by $X'_{C*;C}$ (%) = 100 $(X'_{C*}-X'_C)/X'_C$.

The SPSS® software for statistical analysis was applied for the processing of the experimental data. In the statistical analysis of the group mean values X'_{P*} vs. X'_P and X'_P vs. X'_{N*}, we performed separate one-way ANOVAs for each measured brain region, following the Levene-test of homogenity of the variances. Normal distributions were calculated using Blom's proportional estimation formula and the 'normal P-P plot' routine. For the multiple comparisons, Bonferroni's post-hoc test was applied. Due to the relatively small n in the C- and C*-group (cf. table 1), the non-parametric Wilcoxon-test was applied to compare X'_{C*} vs. X'_C. Both tests consider small differences in the n values of compared groups. The significances shown in figures 8A, B; 9A, B; 10A, B result from the statistical analyses of the group mean values.

Results

In a previous study the dose/effect relationships of APO on the prey-catching activity in common toads untreated with APO and in toads 20 min after administration of APO at various doses were investigated [fig. 2, Glagow and Ewert, 1997a]. With an increasing dose of APO, the toads' turning frequency in response to the prey stimulus progressively decreased, whereas the snapping rate increased up to 40 mg/kg. At a dose of APO of 40 mg/kg body wt., orientational turning towards the prey stimulus mostly failed to occur, whereas the facilitation of prey snapping was maximal. The lack of prey-oriented turning and lunging influenced the snapping pattern in a rigid and stereotyped manner [for further details see Glagow and Ewert, 1997a].

Local Cerebral Glucose Utilization
Figure 3A indicates examples of the locations of transverse sections of the toad's brain. Figures 3B and 4a–h are color-coded autoradiographic images of these brain sections from toads without APO treatment (fig. 3Ba, 4A) and after APO treatment (fig. 3Bb, 4B). In various brain structures, the ^{14}C-2DG uptake increases from cold (blue) to warm
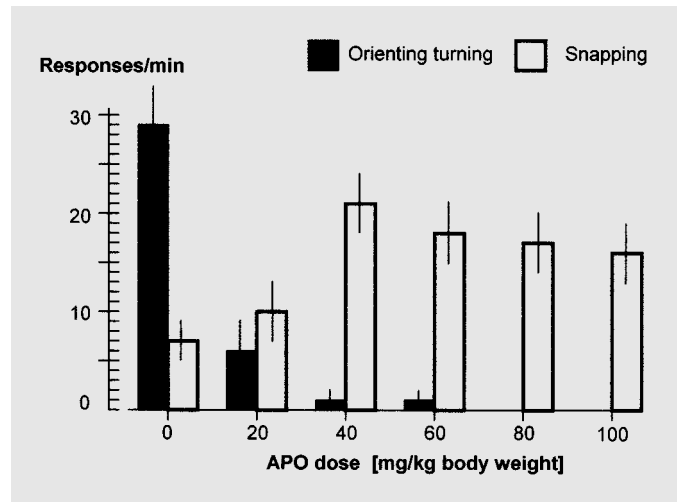
Fig. 2. Influence of intralymphatically administered apomorphine (APO) on the average prey-oriented turning and snapping activities ($\pm SD$) in common toads *Bufo bufo* (n = 15) depending on the dose of APO. Prey-catching activities were measured in a group of toads given no APO and in groups of toads 20 min after administration of APO of different doses [adapted from Glagow and Ewert, 1997a].

(dark red) colors. Figures 5–10 quantitatively show APO-induced glucose utilization that were examined in 41 brain structures. These figures indicate the group mean values X'_{P*}, X'_P, X'_{N*}, X'_{C*}, and X'_C, (fig. 5–7) and show comparisons among different groups (fig. 8–10). In the latter case, we compared P*-group toads (stimulated with prey after APO administration) and P-group toads (stimulated with prey without APO administration) or N*-group toads (stimulated with non-prey after APO administration) and P*-group toads (fig. 8A–10A). Furthermore, we compared C*-group toads (in the absence of prey after APO administration) and C-group toads (in the absence of prey without APO administration) (fig. 8B–10B). These alterations are expressed by the values $X'_{P*;P}$ (%), $X'_{P*;N*}$ (%), and $X'_{C*;C}$ (%), respectively.

Of the 41 brain structures (shown in fig. 8–10), 32 structures displayed statistically significant increases in glucose utilization, 8 structures showed significant decreases, and one structure showed no significant alteration in glucose utilization.

APO-Treated vs. Untreated Prey-Stimulated Groups
In this examination, we compare the $X'_{P*;P}$ (%) values of glucose utilization in the brains of prey-stimulated toads in the APO-treated vs. untreated groups. This is the most relevant comparison for the discussion of the two most unam-

biguous observations with APO treatment, namely, the suppressed orientational turning and locomotion and the increased oral activity compared to untreated common toads (cf. table 1). The comparisons are based on a statistical analysis of the group mean values X'_{P*} and X'_P (see Materials and Methods) [$X'_{P;C}$- and $X'_{N;C}$-values, i.e. the alteration in glucose utilization of APO-untreated toads, in response to different visual stimuli, was described in detail by Finkenstädt et al., 1985, 1986].

Telencephalon

Olfactory Bulb. After administration of APO, the ventral area of the main olfactory bulb (vOB) showed a stronger increase in glucose utilization than the medial area (mOB; fig. 4Ba, 8A). In the accessory olfactory system (AOS), the APO-induced elevation in glucose utilization was larger than any other brain structure investigated (fig. 8A).

Pallium. The rostral dorsal pallium (DP), the posterior two thirds of the lateral pallium (pLP), the lateral prominence (LPR), the posterior dorsal medial pallium (dMP), and the ventral two thirds of the medial pallium (vMP) showed moderately increased glucose utilization under APO treatment (fig. 4Bb, 8A).

Subpallium. Glucose utilization increased in the medial septum (MS), the lateral septum (LS), and the nucleus accumbens (AC) adjacent to the lateral septum, in contrast to the lateral amygdalae (AL) and the ventral striatum (vSTR), which actually showed decreases in glucose utilization (fig. 4Bb, 8A). The anterior entopeduncular nucleus (Ea) displayed an increase.

In the telencephalon, the structures vOB, AOS, LPR, dMP, MS, and LS showed the strongest group mean values in glucose utilization under APO treatment, whereas vSTR and AL displayed the weakest ones (fig. 5A).

Diencephalon

Anterior Dorsal Structures. Under APO treatment, the increase in glucose utilization was strong in the anterior thalamic nucleus (A; fig. 9A). Moderate increases were observed in the complex of the nucleus of Bellonci and the dorsal zone of the ventrolateral thalamic nucleus (NB/VLd) and the lateral anterior thalamic nucleus (La; fig. 4Bc, 9A). The habenular nucleus (HAB) displayed a significant decrease in glucose utilization (fig. 9A).

Ventral Thalamus. Increases in glucose utilization were observed both in the ventromedial nucleus (VM) and the ventral zone of the ventrolateral nucleus (VLv; fig. 4Bc, 9A).

*Preoptic, Hypothalamic and Adjacent Regions.* Glucose utilization increased in the nucleus of the periventricular organ (NPO), the suprachiasmatic nucleus (SCN), and the periventricular region of the dorsal hypothalamus (dHYP; fig. 4Bd, 9A). However, glucose utilization decreased in the preoptic area (PO). The decrease in the ventral hypothalamus (vHYP) was not statistically significant (fig. 4Bd, 9A).

Pretectal Nuclei. The posterior (P) and the lateral posteroventral (Lpv) thalamic nuclei showed increases in glucose utilization; these increases were even stronger in the lateral posterodorsal nucleus (Lpd; fig. 4Bd, 9A).

Fig. 3. A Examples of transverse sections of the common toad's brain, running from rostral (a) to caudal (h). These sections are shown as color-coded autoradiographic images below (B) and in fig. 4AB, a–h. **B** Pattern of ^{14}C-2DG uptake in the optic tectum (OT) of normal, untreated toads stimulated with the 4×28 mm^2 worm-like moving prey dummy [Group-P] and in prey-stimulated toads after APO administration [Group-P*]; TEG, tegmentum; III, 3rd ventricle. Top: representative example of a section through the rostral mesencephalon at level d* (cf. fig. 3A) of a toad of each group. Bottom: Cut-out of the lateral right tectum of the Group-P toad (a), the Group-P* toad (b), and, for comparison, of a histological Klüver-Barrera stain showing the tectal layers 1 (periventricular) to 9 (superficial) and the laminae A–G (c); the regions dOT (dorsal tectum), mOT (medial tectum) and vOT (ventral tectum) refer to the quantitative measurements of ^{14}C-2DG uptake as shown in figures 7 to 10. For the interpretation of the pattern of ^{14}C-2DG uptake in the tectum, the following morphological data are important. The fibers of the contralateral retinal ganglion cells terminate continously in the laminae A through F of layer 9 and in lamina G. A hidden stratification exists, which is masked when terminal degeneration studies are used to study retino-tectal projections [Lázár, 1984]. Assignments of the fiber terminals of the classes of retinal ganglion cells to tectal laminae suggest that class (R1 and) R2 neurons project mainly to laminae A and B including the upper part of C, class R3 neurons project to laminae C–F, and class R4 neurons to laminae F and G [Székely and Lázár, 1976; Ewert, 1997]. Ipsilateral pretectal inputs arrive at layers 8 and 9 [Lázár, 1984; Kozicz and Lázár, 1994; Buxbaum-Conradi and Ewert, 1995]. Ipsilateral thalamic, hypothalamic, and tegmental fibers terminate mainly in layers 3 and 5, and striatal fibers terminate in layer 7 [Wilczynski and Northcutt, 1983b; Lázár, 1984; González and Smeets, 1991; Marín et al., 1997e]. Tectal efferents are mediated by layer 7 and the most upper part of layer 6 [Székely and Lázár, 1976; Weerasuriya and Ewert, 1981; Lázár, 1984]. Calibration bar: 250 µm.

Fig. 4. Color-coded autoradiographic images of brain transverse sections (cf. fig. 3) showing local cerebral uptake of ^{14}C-2DG in APO-untreated toads (**A**) [P-group] and in APO-treated toads (**B**) [P*-group] in response to the 4×28 mm^2 worm-like moving prey stimulus (cf. fig. 1). The radioactivity increases from cold (blue) to warm (red) colors. Examples of brain sections at the levels a–h as shown in figure 3A: (a) olfactory bulbs; (b) medio-caudal telencephalon; (c) diencephalon; (d) caudal diencephalon and rostral mesencephalon; (e) medial mesencephalon; (f) cerebellum and rostral medulla oblongata; (g) medial medulla oblongata; (h) caudal medulla oblongata. Note that the brain sections are reproduced at different magnification. [Nomenclature after Wilczynski and Northcutt, 1977, 1983a, b; Neary and Wilczynski, 1980; Neary and Northcutt, 1983.]
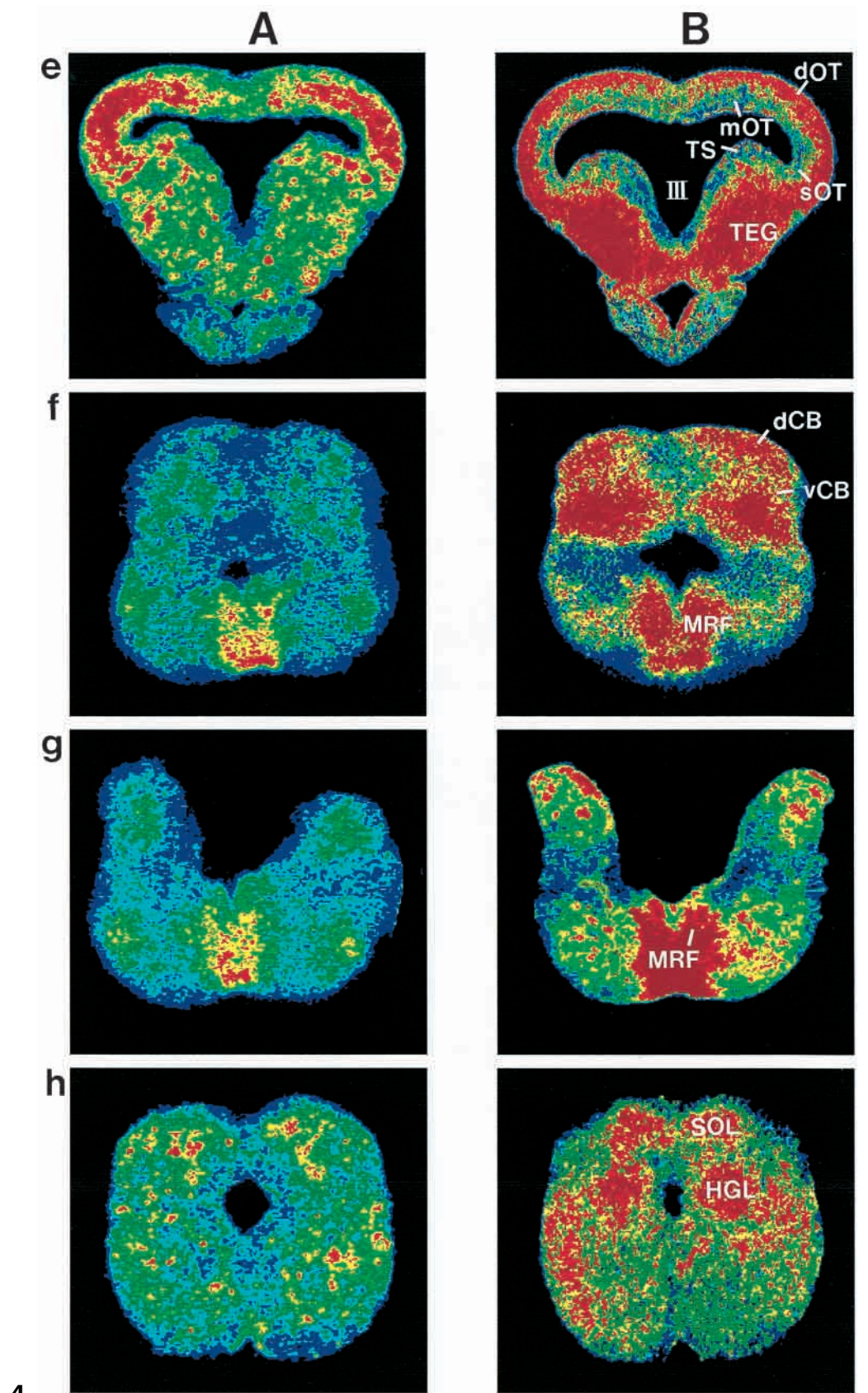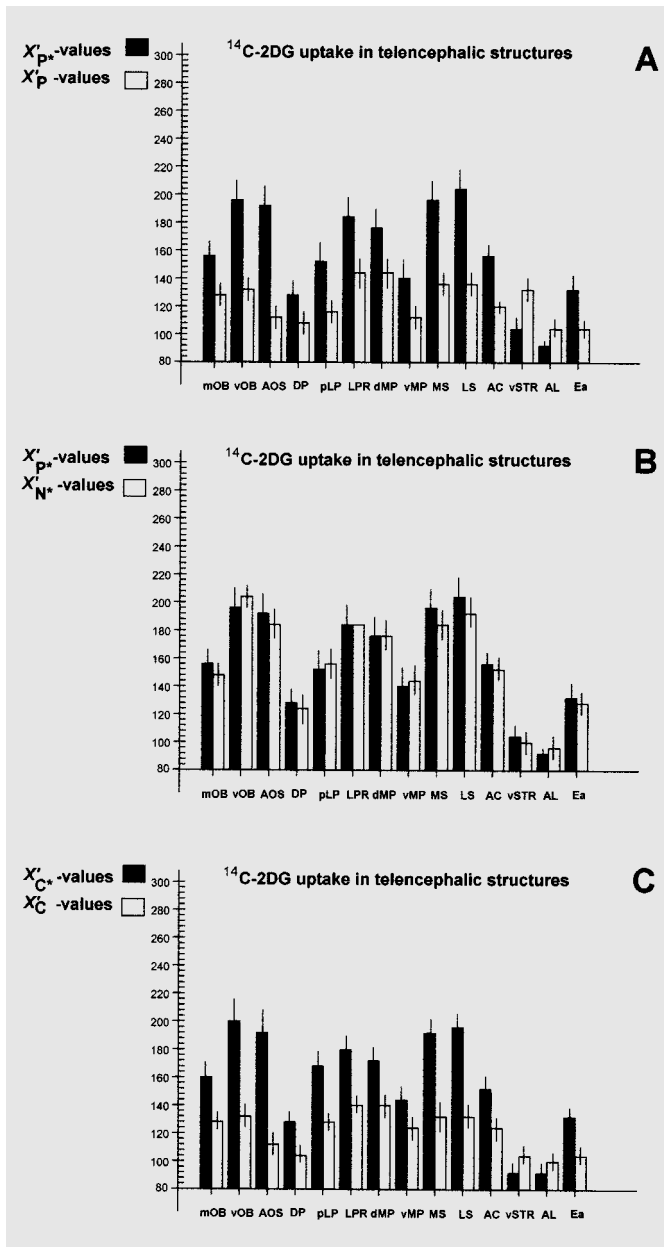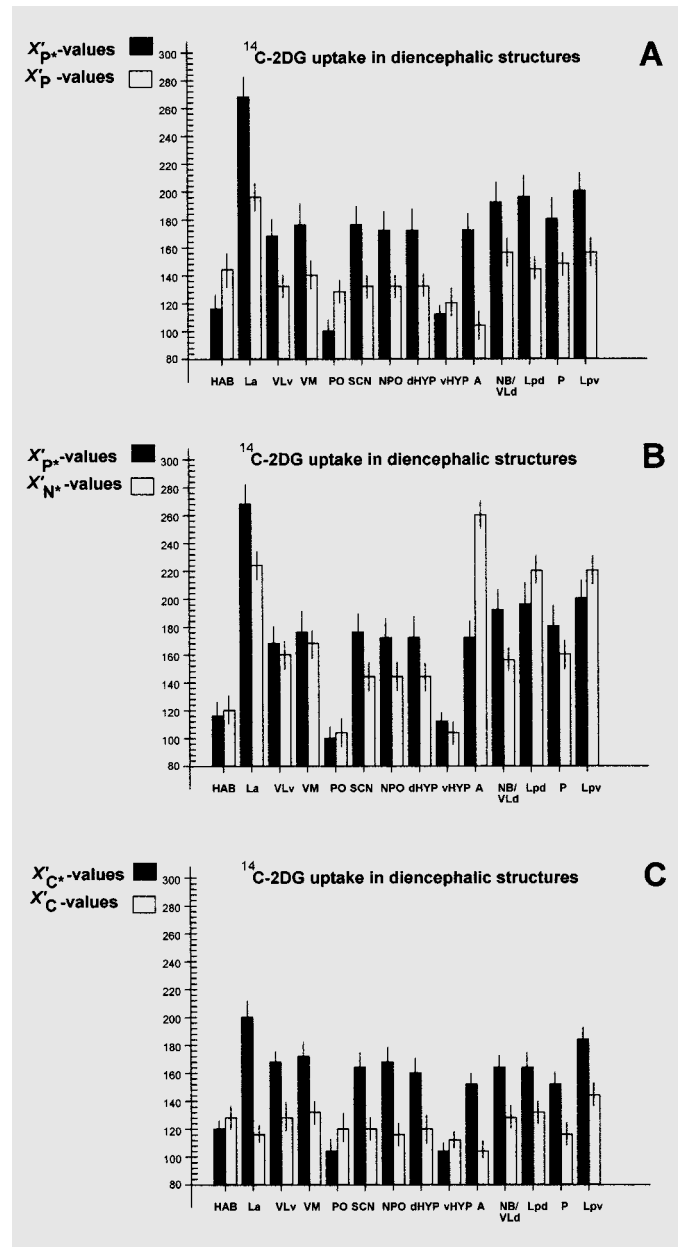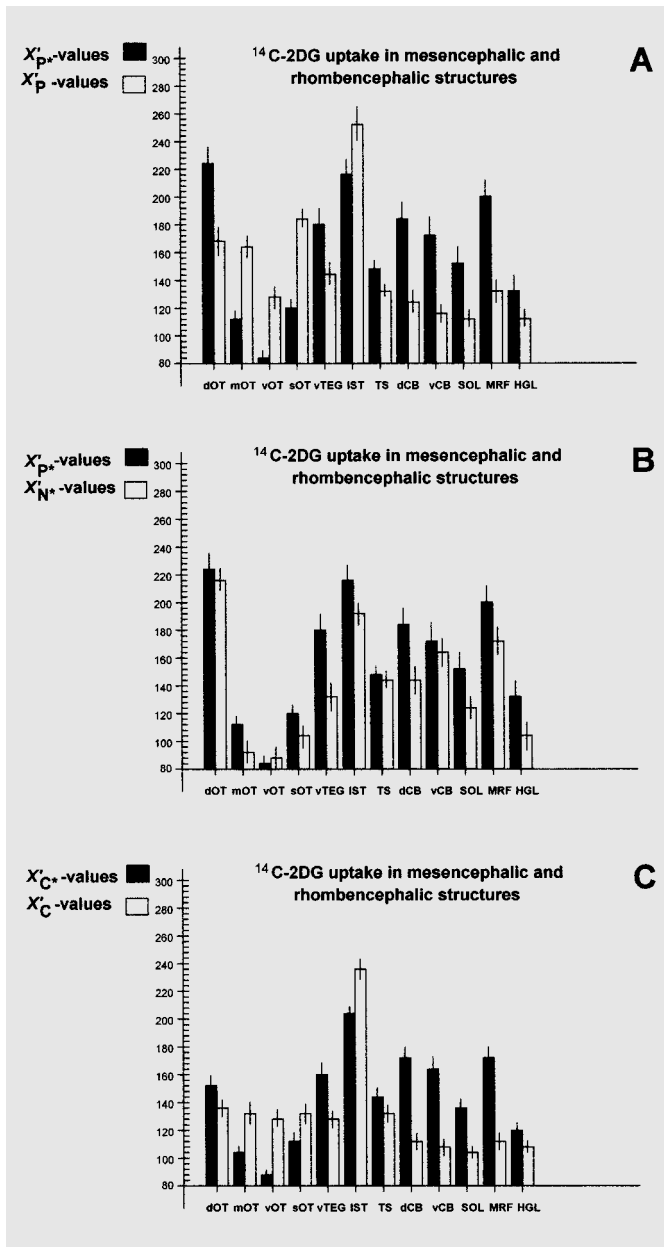
4
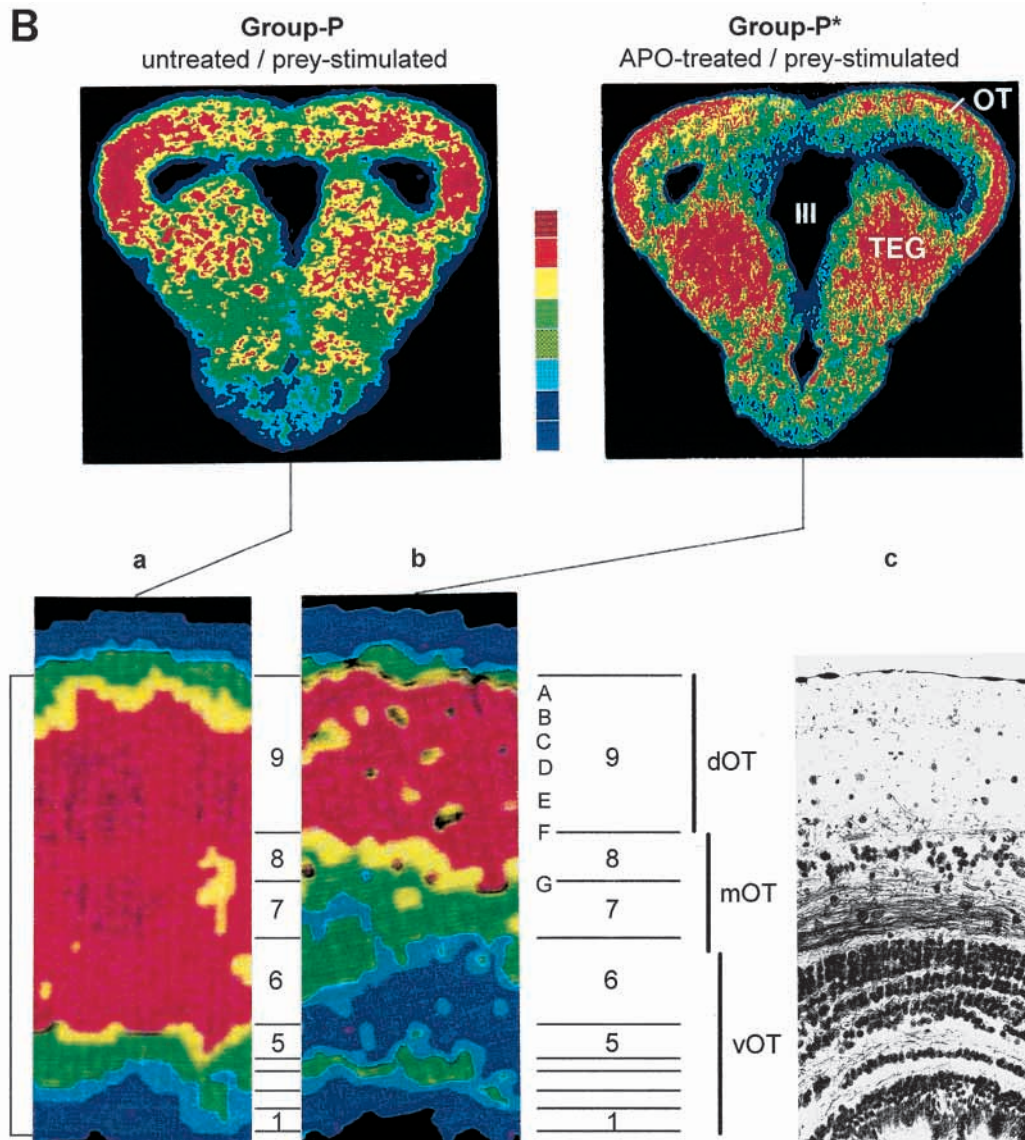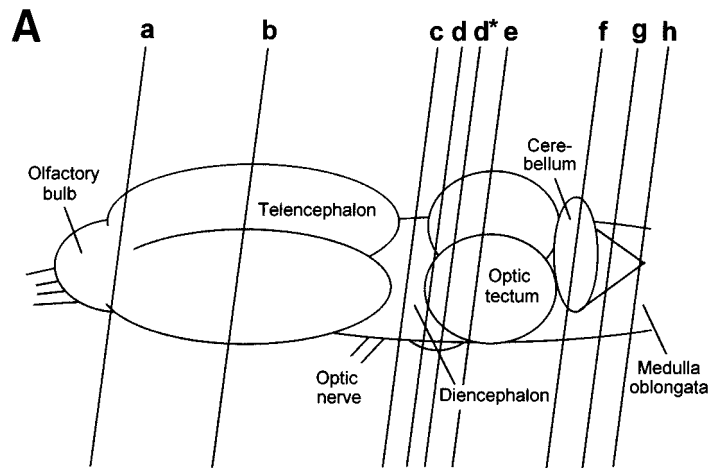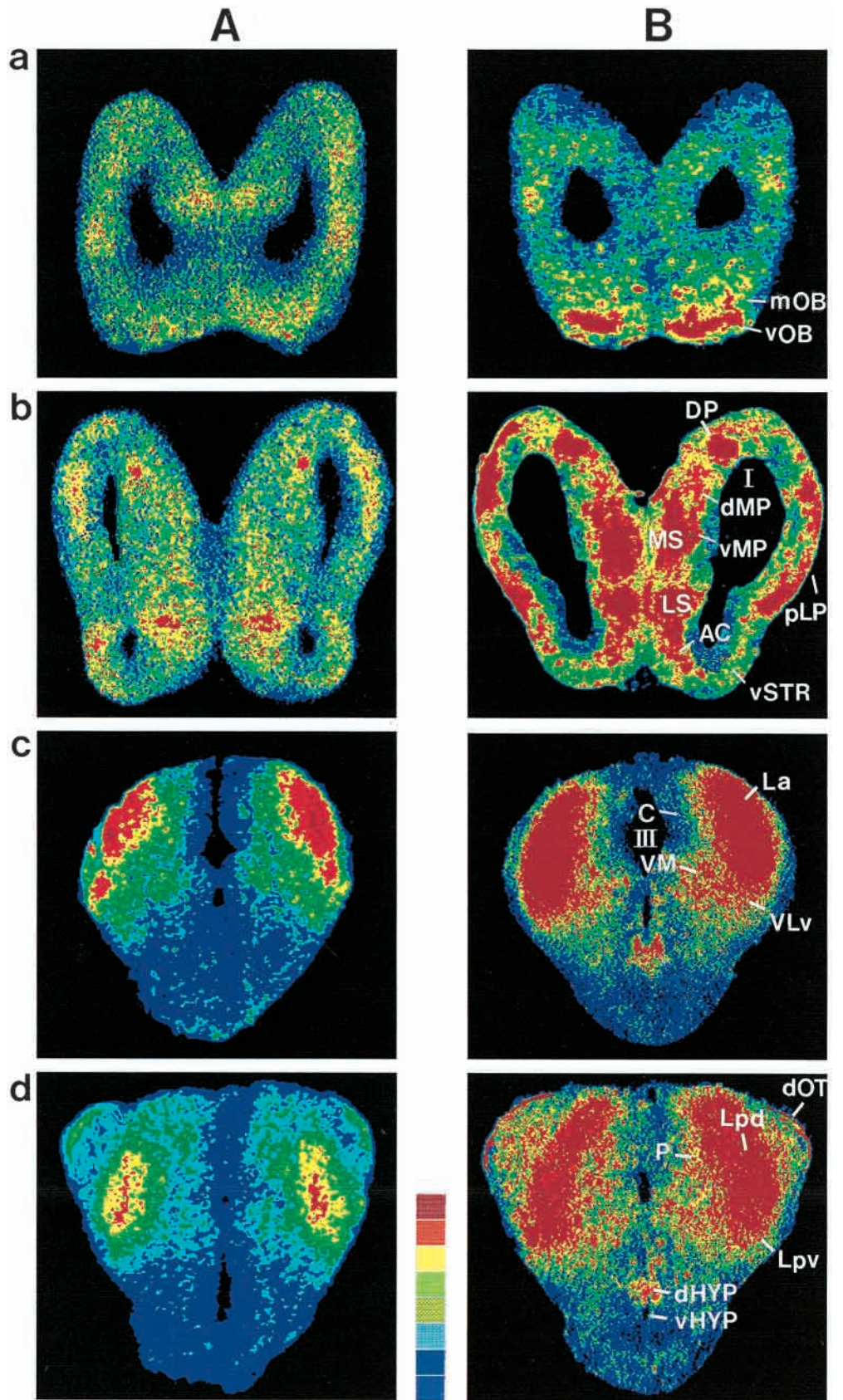
4 (For legend, see p. 228.)

Fig. 5. Average local uptake of ^{14}C-2DG by telencephalic structures in **A**: APO-untreated toads visually stimulated with the worm-like prey dummy [X′$_P$-values of P-group] and APO-treated toads stimulated with the worm-like prey dummy [X′$_{P*}$-values of P*-group], **B**: APO-treated toads visually stimulated with an antiworm non-prey object [X′$_{N*}$-values of N*-group] and, for comparison, APO-treated toads stimulated with the worm-like prey dummy [P*-group], and **C**: APO-untreated toads not visually stimulated [X′$_C$-values of C-group] and APO-treated toads not visually stimulated [X′$_{C*}$-values of C*-group]; mean values ± SD.
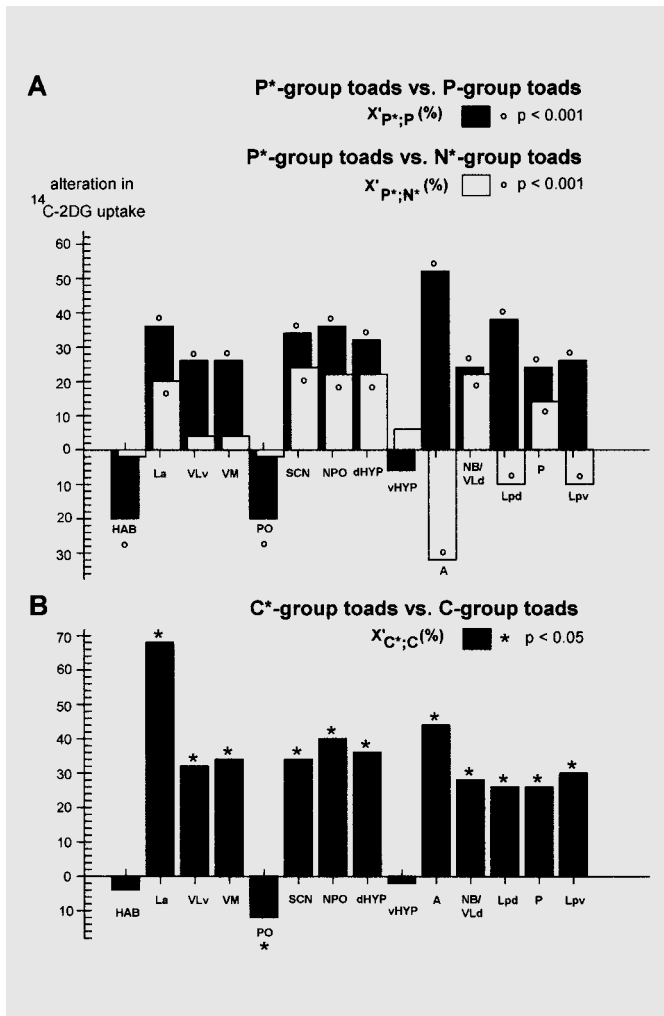
Fig. 6. Average local uptake of ^{14}C-2DG by diencephalic structures in **A**: APO-untreated toads visually stimulated with the worm-like prey dummy [X′$_P$-values of P-group] and APO-treated toads stimulated with the worm-like prey dummy [X′$_{P*}$-values of P*-group], **B**: APO-treated toads visually stimulated with an antiworm non-prey object [X′$_{N*}$-values of N*-group] and, for comparison, APO-treated toads stimulated with the worm-like prey dummy [P*-group], and **C**: APO-untreated toads not visually stimulated [X′$_C$-values of C-group] and APO-treated toads not visually stimulated [X′$_{C*}$-values of C*-group]; mean values ± SD.

Fig. 7. Average local uptake of ^{14}C-2DG by mesencephalic and rhombencephalic (cerebellar and medullary) structures in **A**: APO-untreated toads visually stimulated with the worm-like prey dummy [X'_P-values of P-group] and APO-treated toads stimulated with the worm-like prey dummy [X'_{P*}-values of P*-group], **B**: APO-treated toads visually stimulated with an antiworm non-prey object [X'_{N*}-values of N*-group] and, for comparison, APO-treated toads stimulated with the worm-like prey dummy [P*-group], and **C**: APO-untreated toads not visually stimulated [X'_C-values of C-group] and APO-treated toads not visually stimulated [X'_{C*}-values of C*-group]; mean values ± SD.
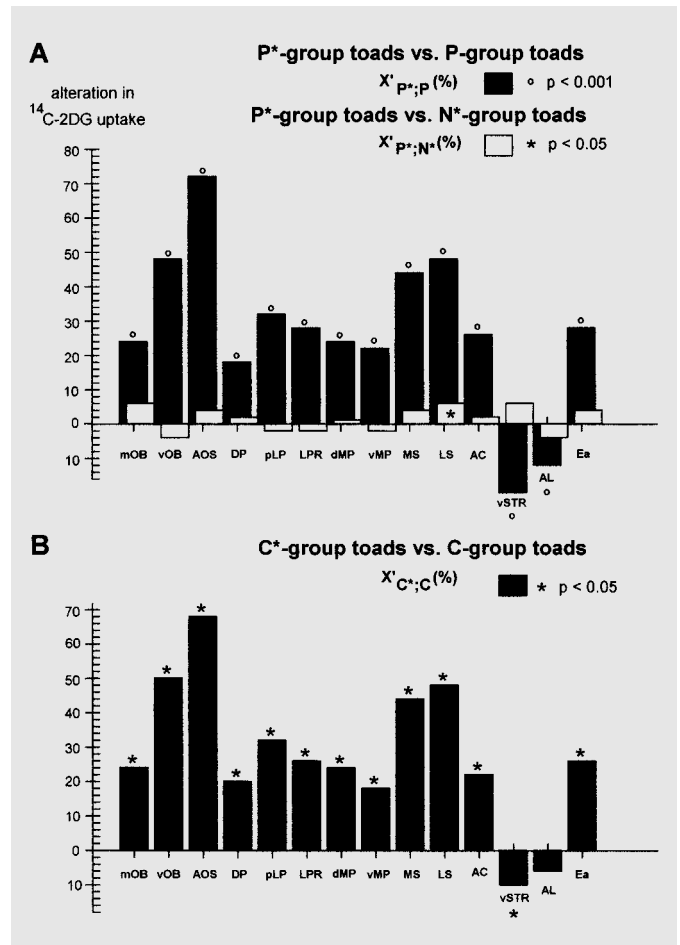
Fig. 8. Average local alteration of ^{14}C-2DG uptake by telencephalic structures in **A**: P*-group vs. P-group toads, the differences in uptake being plotted by the $X'_{P*;P}$ (%) values, and P*-group vs. N*-group toads, plotted by $X'_{P*;N}$ (%), and **B**: C*-group vs. C-group toads, plotted by $X'_{C*;C}$ (%).
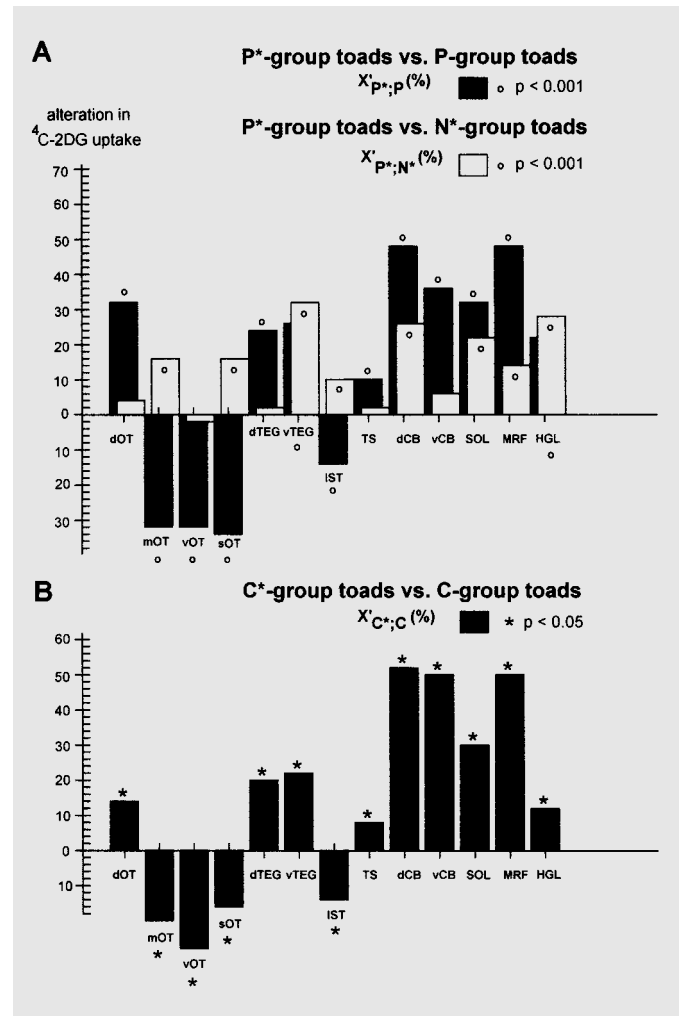
Fig. 9. Average local alteration of ^{14}C-2DG uptake by diencephalic structures in **A**: P*-group vs. P-group toads, the differences in uptake being plotted by the $X'_{P*;P}$ (%) values, and P*-group vs. N*-group toads, plotted by $X'_{P*;N*}$ (%), and **B**: C*-group vs. C-group toads, plotted by $X'_{C*;C}$ (%).

Fig. 10. Average local alteration of ^{14}C-2DG uptake by mesencephalic and rhombencephalic structures in **A**: P*-group vs. P-group toads, the differences in uptake being plotted by the $X'_{P*;P}$ (%) values, and P*-group vs. N*-group toads, plotted by $X'_{P*;N*}$ (%), and **B**: C*-group vs. C-group toads, plotted by $X_{C*;C}$ (%).

In the diencephalon, the La nucleus showed the strongest and the PO area the weakest group mean values in glucose utilization under APO treatment (fig. 6A). The value in the La nucleus was strongest in comparison to all the other brain nuclei investigated after administration of APO (cf. fig. 6A and fig. 5A, 7A).

Mesencephalon

Optic Tectum. The laminar organized optic tectum can be subdivided into dorsal (layer 9), medial [layers 6 (top), 7 and 8], and ventral (layers 1–6) formations (fig. 3Bc). After APO administration, glucose utilization increased in the dorsal formation (dOT), but decreased in the medial (mOT) and ventral (vOT) formations (fig. 3Bb, 4Be, 10A). A decrease in glucose utilization was also observed in the sOT of the mOT, an area of the optic tectum responsible for evoking snapping behavior [Ewert, 1984].

Tegmentum. APO-induced increases in glucose utilization were observed both in the ventral tegmentum (vTEG) and the dorsal tegmentum (dTEG; fig. 3B, 4Be, 10A).

Nucleus Isthmi. The glucose utilization was relatively strong in the isthmic region (IST; fig. 7A). After administration of APO, however, glucose utilization was decreased (fig. 10A).

Torus Semicircularis. A weak increase in glucose utilization was found in the torus (TS; fig. 4Be, 10A).

Cerebellum and Medulla Oblongata

Cerebellum. APO-induced increases in glucose utilization were relatively strong in the dorsal area of the cerebellum (dCB) and moderate in the ventral area (vCB; fig. 4Bf, 10A).

Medulla Oblongata. The increase in glucose utilization was relatively strong in the medial reticular formation (MRF) and moderate in the nucleus of the solitary tract (SOL) and the hypoglossal nucleus (HGL; fig. 4Bg, 4Bh, 10A).

In the mesencephalon/rhombencephalon, the structures dOT, IST, and MRF showed the strongest group mean values in glucose utilization under APO treatment, whereas mOT and vOT displayed the weakest ones (fig. 7A). The value in vOT was weakest in comparison to all the other brain nuclei investigated under APO treatment (cf. fig. 5A, 6A).

Evaluation of the Test and Control Groups

In evaluating the alterations in glucose utilization, it is important to consider that the five experimental groups differed in several ways (cf. table 1): the presence or absence of APO, the presence or absence of prey stimuli, the pattern of the visual stimulus (prey or non-prey), the stimulus frequency, and the behavioral response (orienting, snapping). In the P-group, the APO-untreated toads showed both prey oriented turning and snapping responses. However, the orienting activity was relatively high by comparison with the snapping rate. In the P*-group, the APO-treated toads snapped very frequently when the stimulus traversed a frontal section of the visual field, however, orientational turning behavior failed to occur. Because toads of the P-group maintained orientation to the circling prey stimulus, the net amount of visual stimulation was larger than in the P*-group. In the N*-group, the APO-treated toads snapped only occasionally if the stimulus traversed the frontal field of vision. In the C*- and C-groups the sitting toads received no moving visual stimulus at all. This variability raises the question of whether alterations in glucose utilization resulted from the influences of APO, the visual stimulus and its frequency, or the motor responses. These potentially confounding variables can be evaluated by comparison of the various group mean values.

It is important to note that the general pattern of the $X'_{P*;P}$ values resemble the $X'_{C*;C}$ values in most brain structures (cf. fig. 8A, B; 9A, B; 10A, B). Actually, among the investigated telencephalic structures (fig. 8A, B), the $X'_{P*;P}$ and $X'_{C*;C}$ pairs are mostly congruent. This confirms that the alterations in glucose utilization were APO-induced. This conclusion is further supported by a statistical comparison of the X'_{P*} values with the X'_{N*} values (fig. 8A–10A). We found that the values deviate from each other in only one of the telencephalic structures: the lateral septum (LS; fig. 8A). However, the small difference was at the limit of statistical significance. This suggests that in most telencephalic structures the measured changes in local glucose utilization do not result either from the type of visual stimulus (prey vs. non-prey) or the frequency of snapping (cf. table 1).

Furthermore, strong statements can be made about brain structures that are known to be strictly visual in nature, whereas for others, such as the dorsal hypothalamus or cerebellum, the interpretation of the data becomes more of a problem. In the medial tectal layers (mOT) and the tectal snapping evoking area (sOT), the statistical analysis showed that $X'_{P*} > X'_{N*}$ (fig. 10A). This suggests a difference in the activity of prey-selective tectal neurons [cf. Ewert, 1997] when compared to the P*-group (stimulated with prey) and the N*-group (stimulated with non-prey). Conversely, in the anterior thalamic nucleus (A), the pretectal lateral posterodorsal nucleus (Lpd), and the pretectal lateral posteroventral nucleus (Lpv), the analysis showed that $X'_{N*} > X'_{P*}$ (fig. 9A). This suggests a difference in the activity of neurons that are more sensitive to non-prey (the threatening antiworm stimulus) rather than to prey (the wormlike stimulus) [cf. Ewert, 1997] when the N*-group is compared to the P*-group.

With APO treatment, the anterior thalamic (A), pretectal posterodorsal (Lpd), and dorsal tectal (dOT) retinal projection fields revealed higher levels of glucose utilization in the vision groups (X'_{P*}, X'_{N*}) than in the control group (X'_{C*}) (fig. 6B, C; 7B, C). This suggests general retinal influences. The alterations in glucose utilization in these brain structures, too, looked stronger in the vision group $X'_{P*;P}$ than in the control group $X'_{C*;C}$ (fig. 9A, B; 10A, B). This suggests increased visual activities that are APO-induced.

The tongue-flip controlling hypoglossal nucleus (HGL) indicated an APO-induced stronger glucose utilization in the vision group $X'_{P*;P}$ than in the control group $X'_{C*;C}$ (fig. 10A, B), which is probably associated with the APO-induced increase in the snapping rate of animals observing the prey stimulus. This would explain the significantly increased X'_{P*} value in the HGL when compared to the X'_{N*} value (fig. 10A). The ratio $X'_{P*} > X'_{N*}$ was also detected in the medial reticular formation (MRF; fig. 10A), a component of the bulbar motor system which is involved in snapping pattern generation. We also found such a ratio in the ventral tegmentum (vTEG; fig. 10A), a component of the mesolimbic

system which might be associated with an APO-induced increase in the motivation of snapping. Actually, in the dorsal tegmentum (dTEG; fig. 10A) the X'_{P*} and X'_{N*} values showed no significant difference. The remaining cases in which the X'_{P*} and X'_{N*} values significantly deviate from each other are difficult to interpret.

Discussion

We suggest that dopaminergic effects on various structures of the brain macronetwork (fig. 11) modulate anuran prey-catching patterns in terms of 'hunting' and 'waiting' strategies. Hunting prey involves locomotion, orienting, and snapping. In this strategy, the preying success takes advantage of the animal's mobility but at the risk of being attacked by predators. Waiting for prey safely at a hiding place involves a rather rigid posture. In the waiting strategy, preying success depends on a relatively low snapping threshold, but at the disadvantage of catching non-prey items also. It is possible that species-specific behavioral strategies with tendencies toward hunting (e.g. *Bufo bufo*) and waiting (e.g. *Rana esculenta*) [Eibl-Eibesfeldt, 1951] rely on dose dependent dopaminergic adjustments at different sites in the macronetwork. Such adjustments are probably not fixed, which would allow an individual to select a combination of waiting and hunting behavioral components in response to differing internal and external conditions.

The present investigation was suggested by a previous quantitative study on the dopaminergic modulation of visual responses in common toads [Glagow and Ewert, 1997a] which showed that after systemic administration of the dopamine agonist APO, the mobility in prey-oriented locomotion and turning was reduced (and even suppressed at a dose of APO of 40 mg/kg body wt.), whereas the snapping rate in response to prey was simultaneously increased (fig. 2). APO administration changed the toad's prey-catching behavior from a hunting to a waiting strategy.

Orientational turning and snapping are generated by different bulbar/spinal motor systems which are, in turn, triggered by different tectal channels. Ingle [1983] has shown that the turn-generating system receives its afferents from the crossed tecto-bulbar/spinal pathway (fig. 11; see Ttb/s), whereas the snap-generating system is activated by uncrossed tecto-bulbar fibers (fig. 11; see Ttb). Both pathways contain axons of prey-selective neurons [Ewert, 1984, 1987; Satou and Ewert, 1985]. The autoradiographic data in the current study show that under APO treatment the glucose utilization in the tectal output layers is very low [see also Glagow and Ewert, 1996, 1997b]. Our hypothesis suggests
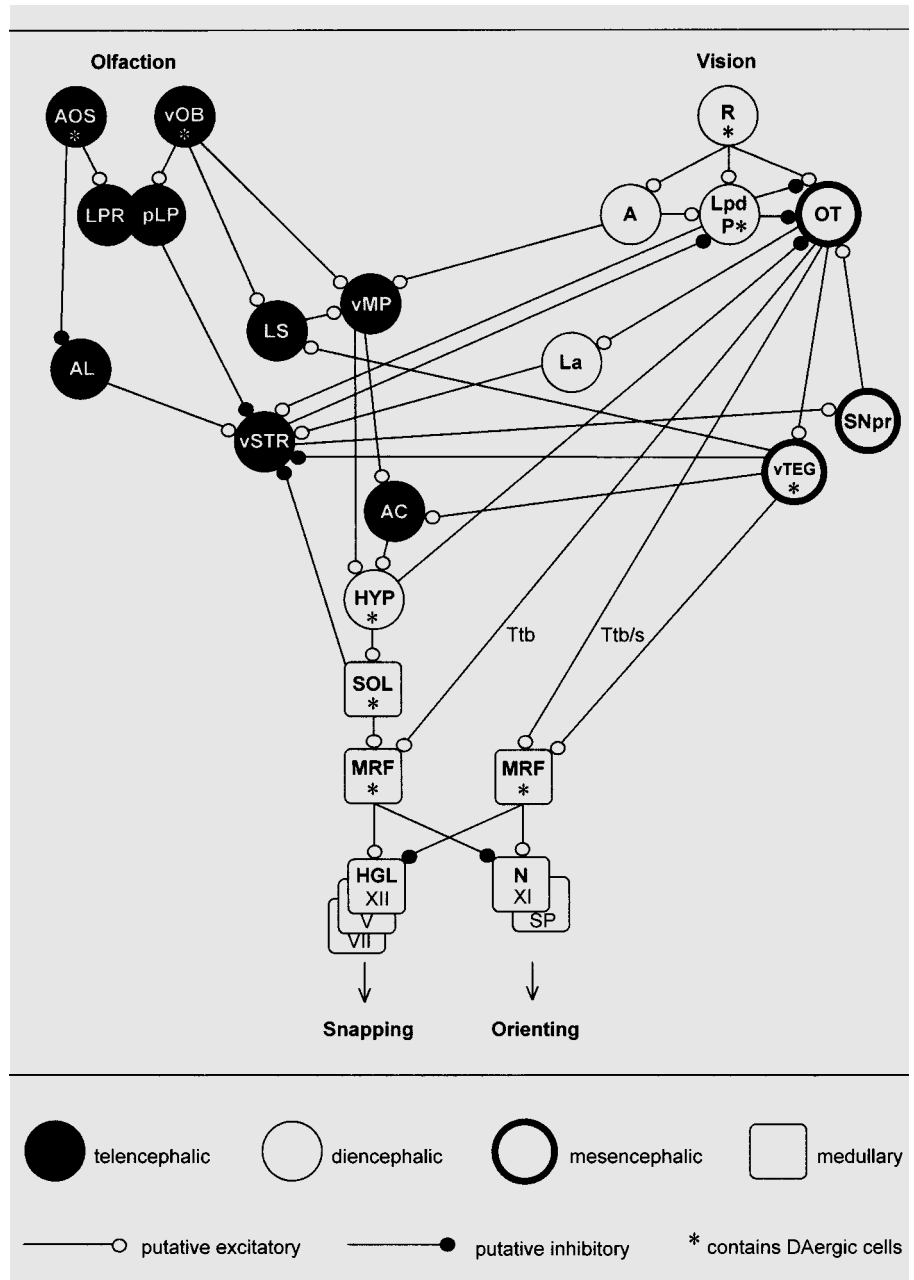
that at the high dose of APO used in this study, the reduced tectal output is subthreshold to trigger the locomotion- and turn-generating networks. However, the reduced tectal output under these conditions is sufficient for the release of augmented stereotyped snapping, assuming that APO modulates the activity of other structures that lower the trigger threshold in the snap-generating network.

Having evaluated the test and control groups, in the following discussion we compare APO-induced alterations of neural activity in various brain structures with the APO-induced behavioral syndrome. The network diagram of figure 11 illustrates several structures and connections which seem to be relevant to this discussion. Figure 12 shows that the brain structures containing dopaminergic cells and/or dopaminergic fibers [Tohyama et al., 1977; Parent and Dubé, 1983; Parent et al., 1984; González and Smeets, 1991; Marín et al., 1997a–e], display APO-induced alterations in glucose utilization so far investigated in this study. APO-induced alterations in other brain structures probably result from their connections to (some of) these dopaminergic cells or fibers (see also fig. 11).

Methodological Considerations

There are limitations to the ^{14}C-2DG method, such as the temporal resolution in functional mapping. The ^{14}C-2DG method is quite useful for spatial resolution, but it has limitations in the temporal dimension in that we can only measure the cumulative changes in ^{14}C-2DG uptake during the 45-min observation period. In the present study, this sort of averaging is regarded as an advantage rather than a disadvantage. Another methodological consideration is the neurophysiological correlates of alterations in ^{14}C-2DG uptake. The ^{14}C-2DG method allows one to monitor the local cerebral glucose utilization in local energy metabolism required for the sodium/potassium pump, particularly in the neuropil. Because we measure changes in ^{14}C-2DG uptake over much more than one second, we can infer correlations between unit activity and the cumulative net metabolic activity. In fact, many examples in the literature show that there is good correlation between the electric and metabolic activity and other activities related to this. Furthermore, postsynaptic inhibition involves the sodium/potassium pump less than postsynaptic excitation, both in the neuropil and in the cell bodies. However, increases and decreases in glucose utilization are not necessarily equivalent to excitation and inhibition, respectively. Presynaptic inhibition, for example, can be accompanied by a relatively high local energy metabolism. Knowledge about the ^{14}C-2DG accumulation pattern must, therefore, be coupled with knowledge about the neuronal unit activity in the region under investigation. The

Fig. 11. Examples of anatomic connections of brain structures that are suggested to be associated with the release and the modulation of prey orienting and snapping in toads after administration of APO. The retinal projection fields in the anterior thalamic nucleus (A), pretectal region (Lpd/P), and optic tectum (OT) receive APO-induced increased retinal inputs due to dopaminergic modulation in the retina (R). The pretectal P nucleus, too, contains dopaminergic cells which rise pretectal activity in the presence of APO. As a result, pretecto-tectal inhibition overrides retino-tectal excitation. Furthermore, APO leads to a decrease in the activity of the ventral striatum, which reduces the gating function of a disinhibitory striato(vSTR)-pretecto(Lpd/P)-tectal(OT) pathway. Consequently, tectal output is dramatically reduced. Tectal efferents travel in the tractus tectobulbaris et spinalis (Ttb/s) to the system responsible for the generation of orienting movements; this system involves the medial reticular formation (MRF), the bulbar nucleus accessorius (N XI), and spinal structures (SP). Tectal efferents travelling in the tractus tectobulbaris (Ttb) reach the snapping generating system that involves another part of the medial reticular formation (MRF), the trigeminal nucleus (N V; innervating the jaw elevator muscle), the facial nucleus (N VII; innervating the jaw depressor muscle), and the hypoglossal nucleus (N XII, HGL; innervating the tongue protractor and retractor muscles). It is suggested that the APO-induced decreased tectal output is subliminal to trigger orientational turning toward prey; however, the reduced tectal output is sufficient to trigger snapping toward prey. The increase in the snapping rate after administration of APO can be explained by level setting of the snapping generating system due to excitatory indirect inputs from the forebrain: [1] Olfactory projection fields – the lateral prominence (LPR), the posterior lateral pallium (pLP), the septum (LS), and the ventromedial pallium (vMP) – receive APO-induced increased sustained inputs due to dopaminergic modulations in the ventral main olfactory bulb (vOB) and the accessory olfactory system (AOS); [2] the ventral medial pallium as a significant part of the limbic system integrates, on the one hand, inputs from the olfactory system and the lateral septum and, on the other hand, visual inputs relayed by the anterior thalamic nucleus; [3] the resulting medial pallial output activates – in concert with APO-induced increased output of dopaminergic ventral tegmental structures (vTEG) – the nucleus accumbens (AC) which in turn has access to the snap generating system via hypothalamic (HYP) and solitary (SOL) structures. There is also a direct pathway from vMP to HYP. See list of abbreviations.

[The connections shown in this diagram are derived from neuroanatomic studies by Rubinson, 1968; Lázár, 1969, 1971; Hoffmann, 1973; Kokoros, 1973; Gruberg and Ambros, 1974; Kicliter and Northcutt, 1975; Northcutt and Royce, 1975; Scalia and Colman, 1975; Scalia, 1976a, b; Kicliter and Ebbesson, 1976; Székely and Lázár, 1976; Wilczynski and Northcutt, 1977; Kicliter, 1979; Ronan and Northcutt, 1979; Neary and Wilczynski, 1979, 1980; Northcutt and Kicliter, 1980; Neary and Northcutt, 1983; Székely et al., 1983; Weerasuriya and Ewert, 1983; Wilczynski and Northcutt, 1983a, b; Weerasuriya, 1989; González and Smeets, 1991; Kozicz and Lázár, 1994; Marín et al., 1997a–d; 1998.]

Fig. 12. Comparison between dopaminergic (or dopaminergically innervated) brain structures and glucose utilization after systemic administration of APO in anurans. This figure lists the names of brain structures that contain dopaminergic cell bodies (top) and/or dopaminergic fibers (bottom). Structures on white background showed an APO-induced increase in glucose utilization and structures on black background showed an APO-induced decrease. From González and Smeets [1991] and Glagow and Ewert [this study]. For dopaminergic cells in the retina see Djamgoz and Wagner [1992].
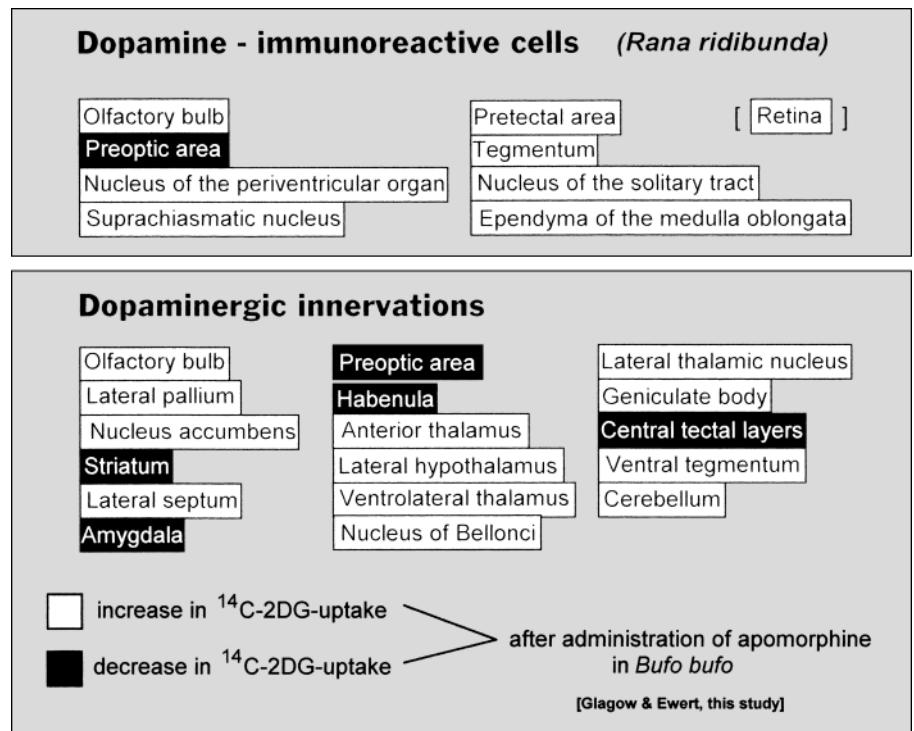
^{14}C-2DG method also provides interesting 'landmarks' for electrophysiological studies.

APO-Induced Suppression of Orienting

In the following section we discuss the APO-induced activity pattern in brain structures which leads to a suppression of prey-oriented turning and locomotion. Structures involved are the retina, the tectum, and the pretectum as components of a stimulus-response mediated releasing system and the striatum and the pretectum as components of its modulating loop [Ewert et al., 1999].

Retinal Output. Electrophysiological recordings of summated field potentials demonstrated that retinal visual output to the superficial tectal projection fields and to the pretectal projection fields is enhanced either after systemic administration of APO or after intraocular administration of APO or dopamine [Röttgen, 1999; Schwippert, unpubl.]. These changes are due to dopaminergic modulation in the retinal network [Djamgoz and Wagner, 1992]. This result is consistent with recordings of action potentials from single fiber endings of retinal ganglion cells in the superficial optic tectum: the discharge rates of these cells in response to moving visual stimuli were significantly increased after systemic administration of APO [Glagow and Ewert, 1997b]. In addition to the tectum and pretectum, there are other pro-jection fields that receive APO-enhanced retinal input, such as the nucleus of Bellonci and the anterior dorsal thalamic nucleus (fig. 11; see R → A, R → Lpd; R → OT) [Lázár, 1971; Fite and Scalia, 1976]. The present ^{14}C-2DG study showed APO-induced increases in glucose utilization in all primary retinal projection fields.

Tectal Output. Although the superficial optic tectum (dOT; as a primary projection field of retinal ganglion cell fibers) displayed strong increases in glucose utilization, the medial tectal layers (mOT; mediating tectal output) showed a strong APO-induced decrease in glucose utilization (fig. 3Bb). This is consistent with APO-induced decreases in the visual discharge rates of tectal prey selective neurons – recorded from medial tectal layers 6 (top) and 7 by Glagow and Ewert [1997b] – known to project to the medullary motor systems (fig. 11; see OT → MRF via Ttb/s) [Székely and Lázár, 1976; Weerasuriya and Ewert, 1981; Satou and Ewert, 1985; Ewert et al., 1990; Matsumoto et al., 1991]. The APO-induced decrease in both the visual discharge rates of these tectal neurons and the metabolic activity of the respective tectal layers (mOT) correlates well with the APO-induced suppression of prey orienting as shown in behavioral studies by Glagow and Ewert [1997a] (see also fig. 2).

Pretecto-Tectal Inhibition. The main question concerns how an APO-induced increased retinal output leads to a

reduced tectal output. One explanation includes the ipsilateral inhibitory connections from the pretectal Lpd/P nuclei to the optic tectum (fig. 11; see Lpd/P → OT) in which increased retinal inputs to the contralateral pretectum and tectum could lead to an attenuation of tectal output. For evidence of inhibitory pretecto-tectal influences see Ewert [1968], Ingle [1973], Ewert et al. [1974, 1996], Kozicz and Lázár [1994], Chapman and Debski [1995], Schwippert and Ewert [1995], and Schwippert et al. [1998]. Pretecto-tectal connections were traced anatomically by Wilczynski and Northcutt [1977] and assigned physiologically to pretectal thalamic neurons of the classes TH3 and TH4 by Buxbaum-Conradi and Ewert [1995]. After systemic administration of APO, the visual discharge rates of TH3 and TH4 neurons were enhanced [Glagow and Ewert, 1996], and this is consistent with the increased glucose utilization in pretectal nuclei shown in the present study. Therefore, we suggest that an APO-induced increase in pretectal inhibitory input to the tectum leads to a reduced tectal output.

Striatal Influences. Pretectal structures are connected to, and controlled by, the ventral striatum [e.g. Wilczynski and Northcutt, 1983b; Marín et al., 1997c] (fig. 11). Previous ^{14}C-2DG studies in toads showed a positive correlation of glucose utilization in the caudal ventral striatum with the animal's prey-oriented turning activity [Finkenstädt et al., 1986]. In the present study, in which the prey-oriented turning behavior of toads failed to occur after APO administration, the glucose utilization in the ventral striatum was reduced. This result is in agreement with previous lesion studies showing that prey orienting behavior failed to occur in toads [Finkenstädt, 1989] and frogs [Patton and Grobstein, 1998a, b] after striatal lesions. We suggest that the ventral striatum acts via a disynaptic disinhibitory striato-pretecto-tectal modulatory pathway consisting of two components: a striato-pretectal inhibitory route and a pretecto-tectal inhibitory route (fig. 11; see vSTR → Lpd/P → OT). Activity in (certain) striatal efferent neurons attenuates pretectal activity and along with this the pretecto-tectal inhibitory influences, thus gating the tectal releasing system for prey-oriented turning [Ewert, 1984, 1992, 1997; Ewert et al., 1996, 1999]. Several types of efferent striatal visual cells were described by Buxbaum-Conradi and Ewert [1999]. For striato-pretectal connections see Wilczynski and Northcutt [1983b], Lázár and Kozicz [1990], Marín et al. [1997c], and Matsumoto et al. [1991]. The present study shows that striatal activity was reduced after APO administration, whereas pretectal activity increased. The resulting pretecto-tectal inhibition could then dramatically attenuate tectal output which would explain the suppression of prey-oriented turning behavior. There are other connections by which the amphibian striatum might control tectal responses, such as by a striato-tegmento(nigro)-tectal route (fig. 11; see vSTR → SNpr → OT) [Wilczynski and Northcutt, 1983b; Marín et al., 1997c, 1998a, b].

APO-Induced Facilitation of Snapping

In the following section we discuss the APO-induced activity patterns in brain structures which may be responsible for lowering the trigger threshold of the snap-generating network. APO-induced increases in glucose utilization were observed in the medial reticular formation and in the hypoglossal nucleus, both of which are involved in the motor pattern generation of snapping [Satou et al., 1985; Matsushima et al., 1989; Ewert et al., 1994a]. The increases in glucose utilization in limbic structures (ventromedial pallium, septum, nucleus accumbens) and in structures that are connected to the limbic system (hypothalamus, ventral tegmentum) could be associated with setting the level of snapping motivation [Weerasuriya, 1983; Székely et al., 1983].

The medial pallium ['primordium hippocampi' of Herrick, 1933] is homologous to the mammalian hippocampus and thus constitutes a significant component of the limbic system. The ventro-medial pallium integrates APO-induced increased sustained visual input, relayed by the anterior dorsal thalamic nucleus, and APO-induced increased sustained olfactory input, partly relayed by the lateral septum (fig. 11; see vOB → LS → vMP ← A ← R) [Hoffmann, 1973; Kicliter and Northcutt, 1975; Northcutt and Royce, 1975; Northcutt and Kicliter, 1980; Neary and Wilczynski, 1980]. Previous ^{14}C-2DG studies have shown that activity in the ventral medial pallium is associated with conditioning [see Finkenstädt, 1989; Finkenstädt et al., 1985; Merkel-Harff and Ewert, 1991; Papini et al., 1995; Ewert et al., 1994b, 1999]. The increase in glucose utilization in the ventral medial pallium might also result from the action of APO as a positive reinforcer [e.g. see also Baxter et al., 1974; Cools et al., 1977; Schiff, 1982; Woolverton et al., 1984; Müller et al., 1987; Lindenblatt and Delius, 1988; Burg et al., 1989; Wynne and Delius, 1995]. We suggest that the resulting medial pallial output, in concert with APO-enhanced influences from dopaminergic cells of the ventral tegmental area stimulates the nucleus accumbens and the hypothalamus which, with the nucleus of the solitary tract, then influence the reticular/branchiomotor/hypoglossal system to lower the threshold for snap behavior generation (fig. 11). Thus, the assumption that the reduced tectal visual output after APO administration at a high dose is subliminal for the release of prey-oriented turning, but sufficient for the release of snapping, is not contradictory. Pigeons, for example, showed

stereotyped, compulsive pecking after APO administration even in the absence of visual stimuli [Burg et al., 1989].

Comparisons between Toad and Rat

McCulloch et al. [1982] mapped the cerebral ^{14}C-2DG uptake in rats after systemic administration of APO, and these results can be compared with the data obtained in toads. As a consequence of APO-enhanced retinal output, the rat's superficial superior colliculus showed an increase in glucose utilization, comparable to the increase observed in the toad's homologous structure, the superficial optic tectum (dOT). In rats as in toads, APO-induced elevations in the rates of glucose utilization were observed in the ventral thalamic nucleus, the ventral tegmental area, and in the cerebellum. Both in toads and rats, the habenular nucleus displayed a reduction in glucose utilization after APO administration.

However, there are differences between toad and rat following APO administration in glucose utilization in the structures of the limbic and striatal systems [cf. McCulloch et al., 1982]. In the rat limbic system, glucose utilization after APO administration was unaltered in the hippocampus, nucleus accumbens, and septal nucleus, but increased in the homologous structures of toads. The amygdala showed an APO-induced increase in glucose utilization in the rat and a decrease in the toad.

The mammalian striatum is a further site of action of dopaminergic effects after systemic APO treatment. Although systemic injections of APO have shown increased glucose utilization in the striatum of the rat, in the toad's ventral striatum we observed a decrease. However, Brown and Wolfson [1983] reported that the effect of locally administered dopamine on striatal glucose utilization in rats was complex, as 'DA produced some decreased neural activity local to the canula, but there was some increase in glucose utilization also'.

Acknowledgments

References

Andersen, H., C. Braestrup, and A. Randrup (1975) Apomorphine-induced stereotyped biting in the tortoise in relation to dopaminergic mechanisms. Brain Behav. Evol., *11:* 365–373.

Baxter, B.L., M.J. Gluckman, L. Stein, and R.A. Scerni (1974) Self-injection of apomorphine in the rat: positive reinforcement by a dopamine receptor stimulant. Pharmacol. Biochem. Behav., *2:* 387–392.

Blackburn, J.B., J.G. Pfaust, and A.G. Phillips (1992) Dopamine functions in appetitive and defensive behaviours. Prog. Neurobiol., *39:* 247–279.

Brown, L.L., and L.I. Wolfson (1978) Apomorphine increases glucose utilisation in the substantia nigra, subthalamic nucleus and corpus striatum of rat. Brain Res., *140:* 188–193.

Brown, L.L., and L.I. Wolfson (1983) A dopamine-sensitive striatal efferent system mapped with [^{14}C]deoxyglucose in the rat. Brain Res., *261:* 213–229.

Burg, B., C. Haase, U. Lindenblatt, and J.D. Delius (1989) Sensitization to and conditioning with apomorphine in pigeons. Pharmacol. Biochem. Behav., *34:* 59–64.

Buxbaum-Conradi, H., and J.-P. Ewert (1995) Pretecto-tectal influences I. What the toad's pretectum tells its tectum: an antidromic stimulation/recording study. J. Comp. Physiol. A, *176:* 169–180.

Buxbaum-Conradi, H., and J.-P. Ewert (1999) Responses of single neurons in the cane toad's caudal ventral striatum to moving visual stimuli and tests of striatal efferents. Brain Behav. Evol. (in press).

Chapman, A.M., and E.A. Debski (1995) Neuropeptide Y immunoreactivity of a projection from the lateral thalamic nucleus to the optic tectum of the leopard frog. Vis. Neurosci., *12:* 1–9.

Chu, J., R.E Wilcox, and W. Wilczynski (1994) Pharmacological characterization of D1 and D2 dopamine receptors in *Rana pipiens.* Soc. Neurosci. Abstr., *20:* 167.

Cools, A.R., C.L.E. Broekkamp, and J.M. van Rossum (1977) Subcutaneous injections of apomorphine, stimulus generalization and conditioning: serious pitfalls for the examiner using apomorphine as a tool. Pharmacol. Biochem. Behav., *6:* 705–708.

Costall, B., and R.J. Naylor (1973) The role of telencephalic dopaminergic systems in the mediation of apomorphine-stereotyped behaviour. Eur. J. Pharmacol., *24:* 8–24.

Costall, B., R.J. Naylor, and J.E. Olley (1972) The substantia nigra and stereotyped behaviour. Eur. J. Pharm., *18:* 95–106.

Creese, I., and S. Iversen (1975) The pharmacological and anatomical substrates of the amphetamine response in the rat. Brain Res. Osaka, *83:* 419–436.

Dhawan, B., P.N. Saxena, and G.P. Gupta (1961) Apomorphin-induced pecking in pigeons. Brit. J. Pharmacol., *15:* 285–295.

Djamgoz, M.B.A., and H.-J. Wagner (1992) Localization and function of dopamine in the adult vertebrate retina. Neurochem. Int., *20:* 139–191.

Eibl-Eibesfeldt, I. (1951) Nahrungserwerb und Beuteschema der Erdkröte (*Bufo bufo* L.). Behaviour, *4:* 1–35.

Ewert, J.-P. (1968) Der Einfluß von Zwischenhirndefekten auf die Visuomotorik im Beute- und Fluchtverhalten der Erdkröte (*Bufo bufo* L.). Z. Vergl. Physiol., *61:* 41–70.

Ewert, J.-P. (1984) Tectal mechanisms that underlie prey-catching and avoidance behaviors in toads. *In* Comparative Neurology of the Optic Tectum (ed. by H. Vanegas), Plenum Press, New York, pp. 247–416.

Ewert, J.-P. (1987) Neuroethology of releasing mechanisms: prey-catching in toads. Behav. Brain Sci., *10:* 337–405.

Ewert, J.-P. (1992) Neuroethology of an object features relating algorithm and its modification by learning. Rev. Neurosci., *3:* 45–63.

Ewert, J.-P. (1997) Neural correlates of key stimulus and releasing mechanism: a case study and two concepts. Trends Neurosci., *20:* 332–339.

Ewert, J.-P., T.W. Beneke, E. Schürg-Pfeiffer, W.W. Schwippert, and A. Weerasuriya (1994a) Sensorimotor processes that underlie feeding behavior in tetrapods. *In* Advances in Comparative and Environmental Physiology, Vol. 18: Biomechanics of Feeding in Vertebrates (ed. by V.L. Bels, M. Chardon, and P. Vandevalle), Springer, Berlin, pp. 119–162.

Ewert, J.-P., H. Buxbaum-Conradi, M. Glagow, A. Röttgen, E. Schürg-Pfeiffer, and W.W. Schwippert (1999) Forebrain and midbrain structures involved in prey-catching behaviour of toads: stimulus-response mediating circuits and their modulating loops. *In* The Forebrain in Nonmammalian Vertebrates: Structure, Function, and Evolution (ed. by H.J. ten Donkelaar), Special Issue of Eur. J. Morphol., Vol. 37(2,3), Swets & Zeitlinger, Lisse, pp. 172–176.

Ewert, J.-P., A.W. Dinges, and T. Finkenstädt (1994b) Species-universal stimulus responses, modified through conditioning, re-appear after telencephalic lesions in toads. Naturwiss., *81:* 317–320.

Ewert, J.-P., E.M. Framing, E. Schürg-Pfeiffer, and A. Weerasuriya (1990) Responses of medullary neurons to moving visual stimuli in the common toad: I) Characterization of medial reticular neurons by extracellular recording. J. Comp. Physiol. A, *167:* 495–508.

Ewert, J.-P., F.J. Hock, and A. von Wietersheim (1974) Thalamus/Praetectum/Tectum: retinale Topographie und physiologische Interaktionen bei der Kröte (*Bufo bufo* L.). J. Comp. Physiol., *92:* 343–356.

Ewert, J.-P., E. Schürg-Pfeiffer, and W.W. Schwippert (1996) Influence of pretectal lesions on tectal responses to visual stimulation in anurans: field potential, single neuron and behavior analyses. Acta Biol. Acad. Sci. Hung., *47:* 223–245.

Finkenstädt, T. (1989) Visual associative learning: searching for behaviorally relevant brain structures in toads. *In* Visuomotor Coordination, Amphibians, Comparisons, Models, and Robots (ed. by J.-P. Ewert and M.A. Arbib), Plenum Press, New York, pp. 799–832.

Finkenstädt, T., N.T. Adler, T.O. Allen, S.O.E. Ebbesson, and J.-P. Ewert (1985) Mapping of brain activity in mesencephalic and diencephalic structures of toads during presentation of visual key stimuli: a computer assisted analysis of [14]C-2DG autoradiographs. J. Comp. Physiol., *156:* 433–445.

Finkenstädt, T., N.T. Adler, T.O. Allen, and J.-P. Ewert (1986) Regional distribution of glucose utilization in the telencephalon of toads in response to configurational visual stimuli: a [14]C-2DG study. J. Comp. Physiol., *158:* 457–467.

Fite, K.V., and F. Scalia (1976) Central visual pathways in the frog. *In* The Amphibian Visual System: A Multidisciplinary Approach (ed. by K.V. Fite), Academic Press, New York, pp. 87–118.

Gallistel, C.R., C.T. Piner, T.O. Allen, N.T. Adler, E. Yadin, and M. Negin (1982) Computer assisted analysis of 2-DG autoradiographs. Neurosci. Biobehav. Rev., *6:* 409–422.

Glagow, M., and J.-P. Ewert (1996) Apomorphine induced suppression of prey oriented turning in toads is correlated with activity changes in pretectum and tectum: [14]C-2DG studies and single cell recordings. Neurosci. Lett., *220:* 215–218.

Glagow, M., and J.-P. Ewert (1997a) Dopaminergic modulation of visual responses in toads. I. Apomorphine induced effects on visually directed appetitive and consummatory prey-catching behavior. J. Comp. Physiol. A, *180:* 1–9.

Glagow, M., and J.-P. Ewert (1997b) Dopaminergic modulation of visual responses in toads. II. Influences of apomorphine on retinal ganglion cells and tectal cells. J. Comp. Physiol. A, *180:* 11–18.

González, A., and W.J.A.J. Smeets (1991) Comparative analysis of dopamine and tyrosine hydroxylase immunoreactivities in the brain of two amphibians, the anuran *Rana ridibunda* and the urodele *Pleurodeles waltlii*. J. Comp. Neurol., *303:* 457–477.

Grobstein, P. (1991) Directed movement in the frog: a closer look at a central representation of spacial location. *In* Visual Structures and Integrated Functions (ed. by M.A. Arbib and J.-P. Ewert), Springer, Berlin, pp. 125–138.

Grobstein, P., C. Comer, and S.K. Kostyk (1983) Frog prey capture behavior: between sensory maps and directed motor output. *In* Advances in Vertebrate Neuroethology (ed. by J.-P. Ewert, R.R. Capranica, and D.J. Ingle), Plenum Press, New York, pp. 331–347.

Gruberg, E.R., and V.R. Ambros (1974) A forebrain visual projection in the frog (*Rana pipiens*). Exp. Brain Res., *44:* 187–197.

Herrick, C.J. (1933) The amphibian forebrain VIII: Cerebral hemispheres and pallial primordia. J. Comp. Neurol., *58:* 737–759.

Hoffmann, A. (1973) Stereotaxis atlas of the toad's brain. Acta Anat., *84:* 416–451.

Ingle, D. (1973) Disinhibition of tectal neurons by pretectal lesions in the frog. Science, *180:* 422–424.

Ingle, D.J. (1983) Brain mechanisms of visual localization by frogs and toads. *In* Advances in Vertebrate Neuroethology (ed. by J.-P. Ewert, R.R. Capranica, and D.J. Ingle), Plenum Press, New York, pp. 177–226.

Kicliter, E. (1979) Some telencephalic connections in the frog *Rana pipiens*. J. Comp. Neurol., *185:* 75–86.

Kicliter, E., and S.O.E. Ebbesson (1976) Organization of the 'nonolfactory' telencephalon. *In* Frog Neurobiology (ed. by R. Llinás and W. Precht), Springer, Berlin, pp. 946–972.

Kicliter, E., and G. Northcutt (1975) Ascending afferents to the telencephalon of ranid frogs: an anterograde degeneration study. J. Comp. Neur., *161:* 239–254.

Kokoros, J.J. (1973) Efferent connections of the telencephalon in the toad Bufo marinus, and the tiger salamander, *Ambystoma tigrinum*. PhD Thesis, Case Western Reserve University, Cleveland, Ohio, USA.

Kozicz, T., and G. Lázár (1994) The origin of tectal NPY immunopositive fibers in the frog. Brain Res., *635:* 345–348.

Lázár, G. (1969) Efferent pathways of the optic tectum in the frog. Acta Biol. Acad. Sci. Hung., *20:* 171–183.

Lázár, G. (1971) The projection of the retinal quadrants on the optic centers in the frog: a terminal degeneration study. Acta Morph. Acad. Sci. Hung., *19:* 325–334.

Lázár, G. (1984) Structure and connections of the frog optic tectum. *In* Comparative Neurology of the Optic Tectum (ed. by H. Vanegas), Plenum Press, New York, pp. 185–210.

Lázár, G., and T. Kozicz (1990) Morphology of neurons and axon terminals associated with descending and ascending pathways of the lateral forebrain bundle in *Rana esculenta*. Cell Tiss. Res., *260:* 535–548.

Lindenblatt, U., and J.D. Delius (1988) Nucleus basalis prosencephali, a substrate of apomorphine-induced pecking in pigeons. Brain Res., *453:* 1–8.

Ljungberg, T., and U. Ungerstedt (1977) Different behavioural patterns induced by apomorphine: evidence that the method of administration determines the behavioural responses to the drug. Eur. J. Pharmacol., *46:* 41–50.

Marín, O., A. González, and W.J.A.J. Smeets (1997a) Basal ganglia organization in amphibians: afferent connections to the striatum and the nucleus accumbens. J. Comp. Neurol., *378:* 16–49.

Marín, O., A. González, and W.J.A.J. Smeets (1997b) Basal ganglia organization in amphibians: efferent connections of the striatum and the nucleus accumbens. J. Comp. Neurol., *380:* 23–50.

Marín, O., A. González, and W.J.A.J. Smeets (1997c) Anatomical substrate of amphibian basal ganglia involvement in visuomotor behaviour. Eur. J. Neurosci., *9:* 2100–2109.

Marín, O., A. González, and W.J.A.J. Smeets (1998a) Amphibian basal ganglia control of tectal function: a complex matter [commentary and a reply by J.-P. Ewert]. Trends Neurosci., *21(8):* 336–337.

Marín, O., W.J.A.J. Smeets, and A. González (1997d) Basal ganglia organization in amphibians: catecholaminergic innervation of the striatum and the nucleus accumbens. J. Comp. Neurol., *378:* 50–69.

Marín, O., W.J.A.J. Smeets, and A. González (1997e) Basal ganglia organization in amphibians: development of striatal and nucleus accumbens connections with emphasis on the catecholaminergic inputs. J. Comp. Neurol., *383:* 349–369.

Marín, O., W.J.A.J. Smeets, and A. González (1998b) Evolution of the basal ganglia in tetrapods: a new perspective based on recent studies in amphibians. Trends Neurosci., *21:* 487–494.

Matsumoto, N., W.W. Schwippert, T.W. Beneke, and J.-P. Ewert (1991) Forebrain-mediated control of visually guided prey-catching in toads: investigation of striato-pretectal connections with intracellular recording/labeling methods. Behav. Proc., *25:* 27–40.

Matsushima, T., M. Satou, and K. Ueda (1989) Medullary reticular neurons in the Japanese toad: morphology and excitatory inputs from the optic tectum. J. Comp. Physiol. A, *166:* 7–22.

McCulloch, J., H.E. Savaki, M.C. McCulloch, J. Jehle, and L. Sokoloff (1982) The distribution of alterations in energy metabolism in the rat brain produced by apomorphine. Brain Res., *243:* 67–80.

Merkel-Harff, C., and J.-P. Ewert (1991) Learning-related modulation of toad's responses to prey by neural loops involving the forebrain. *In* Visual Structures and Integrated Functions (ed. by M.A. Arbib and J.-P. Ewert), Springer, Berlin, pp. 417–426.

Möller, H.-G., K. Nowak, and K. Kuschinsky (1987) Studies on interactions between conditioned and unconditioned behavioural responses to apomorphine in rats. Naudyn-Schmiedeberg's Arch. Pharm., *335:* 673–679.

Neary, T.J., and R.G. Northcutt (1983) Nuclear organization of the bullfrog diencephalon. J. Comp. Neurol., *213:* 262–278.

Neary, T.J., and W. Wilczynski (1979) Anterior and posterior thalamic afferents in the bullfrog, *Rana catesbeiana*. Soc. Neurosci. Abstr., *5:* 144.

Neary, T.J., and W. Wilczynski (1980) Descending inputs to the optic tectum in ranid frogs. Soc. Neurosci. Abstr., *6:* 629.

Northcutt, R.G., and E. Kicliter (1980) Organization of the amphibian telencephalon. *In* Comparative Neurology of the Telencephalon (ed. by S.O.E. Ebbesson), Plenum Press, New York, pp. 203–255.

Northcutt, R.G., and G.J. Royce (1975) Olfactory bulb projections in the bullfrog *Rana catesbeiana*. J. Morphol., *145:* 51–268.

Papini, M.R., R.N. Muzio, and E.T. Segura (1995) Instrumental learning in toads *(Bufo arenarum):* reinforcer magnitude and the medial pallium. Brain Behav. Evol., *46:* 61–71.

Parent, A., and L. Dubé (1983) The anatomy of monamine-containing neurons in the amphibian brain. *In* Progess in Nonmammalian Brain Research, Vol. 1 (ed. by G. Nisticò and L. Bolis), CRC Press, Boca Raton, Florida, pp. 25–45.

Parent, A., D. Poitras, and L. Dubé (1984) Comparative anatomy of central monoaminergic systems. *In* Handbook of Chemical Neuroanatomy, Vol. 2. Classical Transmitters in the CNS, Part 1 (ed. by A. Björklund and T. Hökfelt), Elsevier Sci. Publ., Amsterdam, pp. 409–439.

Patton, P., and P. Grobstein (1998a) The effects of telencephalic lesions on the visually mediated prey orienting behavior in the leopard frog *(Rana pipiens)*. I. The effects of complete removal of one telencephalic lobe, with a comparison to the effect of unilateral tectal lobe lesions. Brain Behav. Evol., *51:* 123–143.

Patton, P., and P. Grobstein (1998b) The effects of telencephalic lesions on the visually mediated prey orienting behavior in the leopard frog *(Rana pipiens)*. II. The effects of limited lesions to the telencephalon. Brain Behav. Evol., *51:* 144–161.

Röttgen, A. (1999) Über den Einfluß von Neuropharmaka auf die visuelle Ansprechbarkeit in der retino-tectalen Projektion der Agakröte. Dissertation, Fachbereich Biologie/Chemie, Univ. Kassel, Kassel, Germany.

Ronan, M.C., and R.G. Northcutt (1979) Afferent and efferent connections of the bullfrog medial pallium. Soc. Neurosci. Abstr., *5:* 146.

Rubinson, K. (1968) Projections of the tectum opticum of the frog. Brain Behav. Evol., *1:* 529–561.

Satou, M., and J.-P. Ewert (1985) The antidromic activation of tectal neurons by electrical stimuli applied to the caudal medulla oblongata in the toad *Bufo bufo* L. J. Comp. Physiol. A, *157:* 739–748.

Satou, M., T. Matsushima, H. Takeuchi, and K. Ueda (1985) Tongue-muscle-controlling motoneurons in the Japanese toad: topography, morphology and neuronal pathways from the 'snapping-evoking area' in the optic tectum. J. Comp. Physiol. A, *157:* 717–737.

Scalia, F. (1976a) Structure of the olfactory and accessory olfactory systems. *In* Frog Neurobiology (ed. by R. Llinás and W. Precht), Springer, Berlin, pp. 213–233.

Scalia, F. (1976b) The optic pathway of the frog: nuclear organization and connections. *In* Frog Neurobiology (ed. by R. Llinás and W. Precht), Springer, Berlin, pp. 386–406.

Scalia, F., and D.R. Colman (1975) Identification of telencephalic efferent thalamic nuclei associated with the visual system of the frog. Soc. Neurosci. Abstr., *1:* 65.

Schiff, S.R. (1982) Conditioned dopaminergic activity. Biol. Psychiat., *17:* 135–154.

Schwippert, W.W., and J.-P. Ewert (1995) Effect of neuropeptide-Y on tectal field potentials in the toad. Brain Res., *669:* 150–152.

Schwippert, W.W., A. Röttgen, and J.-P. Ewert (1998) Neuropeptide Y (NPY) or fragment NPY13-36, but not NPY18-36, inhibit retinotectal transfer in cane toads, *Bufo marinus.* Neurosci. Lett., *253:* 33–36.

Sokoloff, L., M. Reivich, C. Kennedy, M.H. Des-Rosiers, C.S. Patlak, K.D. Pettigrew, O. Sakurada, and M. Shinohara (1977) The (^{14}C)-deoxyglucose method for the measurement of local cerebral glucose utilization: theory, procedure and normal values in the conscious and anesthetized albino rat. J. Neurochem., *28:* 897–916.

Székely, G., and G. Lázár (1976) Cellular and synaptic architecture of the optic tectum. *In* Frog Neurobiology (ed. by R. Llinás and W. Precht), Springer, Berlin, pp. 407–434.

Székely, G., G. Levai, and K. Matesz (1983) Primary afferent terminals in the nucleus of the solitary tract of the frog: an electron microscopic study. Exp. Brain Res., *53:* 109–117.

Tohyama, M., K. Yamamoto, Satoh, T. Sakumoto, and N. Shimizu (1977) Catecholamine innervation of the forebrain in the bull frog, *Rana catesbeiana.* J. Hirnforsch., *18:* 223–228.

Wachowitz, S., and J.-P. Ewert (1996) A key by which the toad's visual system gets access to the domain of prey. Physiol. Behav., *60:* 877–887.

Weerasuriya, A. (1983) Snapping in toads: some aspects of sensorimotor interfacing and motor pattern generation. *In* Advances in Vertebrate Neuroethology (ed. by J.-P. Ewert, R.R. Capranica, and D.J. Ingle), Plenum Press, New York, pp. 613–628.

Weerasuriya, A. (1989) In search of the motor pattern generator for snapping in toads. *In* Visuomotor Coordination: Amphibians, Comparisons, Models, and Robots (ed. by J.-P. Ewert and M.A. Arbib), Plenum Press, New York, pp. 589–614.

Weerasuriya, A., and J.-P. Ewert (1981) Prey-selective neurons in the toad's optic tectum and sensorimotor interfacing: HRP studies and recording experiments. J. Comp. Physiol., *144:* 429–434.

Weerasuriya, A., and J.-P. Ewert (1983) Afferents of some dorsal retino-recipient areas of the brain of *Bufo bufo*. Soc. Neurosci. Abstr., *9:* 536.

Wilczynski, W., and R.G. Northcutt (1977) Afferents to the optic tectum of the leopard frog: an HRP study. J. Comp. Neurol., *173:* 219–229.

Wilczynski, W., and R.G. Northcutt (1983a) Connections of the bullfrog striatum: afferent organization. J. Comp. Neurol., *214:* 321–332.

Wilczynski, W., and R.G. Northcutt (1983b) Connections of the bullfrog striatum: efferent projections. J. Comp. Neurol., *214:* 333–343.

Woolverton, W.L., L.I. Goldberg, and J.Z. Ginos (1984) Intravenous self-administration of dopamine receptor agonists by rhesus monkeys. J. Pharmacol. Exp. Ther., *230:* 678–683.

Wynne, B., and J.D. Delius (1995) Sensitization to apomorphine in pigeons: unaffected by latent inhibition but still due to classical conditioning. Psychopharmacol., *119:* 414–420.

Young, W.G., and J.A. Deutsch (1980) Effects of blood glucose levels on (^{14}C)2-deoxyglucose uptake in rat brain tissue. Neurosci. Lett., *20:* 89–93.